

Not All Tasks are Equal - Task Attended Meta-learning for Few-shot Learning

Anonymous authors
Paper under double-blind review

Abstract

1 Meta-learning (ML) has emerged as a promising direction in learning models under con-
2 strained resource settings like few-shot learning. The popular approaches for ML either
3 learn a generalizable initial model or a generic parametric optimizer through batch episodic
4 training. In this work, we study the importance of tasks in a batch for ML. We hypothesize
5 that the common assumption in batch episodic training where each task in a batch has an
6 equal contribution to learning an optimal meta-model need not be true. We propose to
7 weight the tasks in a batch according to their “importance” in improving the meta-model’s
8 learning. To this end, we introduce a training curriculum called task attended meta-training
9 to learn a meta-model from weighted tasks in a batch. The task attention module is a stan-
10 dalone unit and can be integrated with any batch episodic training regimen. Comparison of
11 task-attended ML models with their non-task-attended counterparts on complex datasets,
12 performance improvement of proposed curriculum over state-of-the-art task scheduling algo-
13 rithms on noisy datasets, and cross-domain few shot learning setup validate its effectiveness.

14 1 Introduction

15 The ability to infer knowledge and discover complex representations from data has made deep learning models
16 widely popular in the machine learning community. However, these models are data-hungry, often requiring
17 large volumes of labeled data for training. Collection and annotation of such large amounts of training data
18 may not be feasible for many real life applications, especially in domains that are inherently data constrained,
19 like medical and satellite image classification, drug toxicity estimation, etc. Meta-learning (ML) has emerged
20 as a promising direction for learning models in such settings, where only a limited amount (few-shots) of
21 labeled training data is available. A typical ML algorithm employs an episodic training regimen that differs
22 from the training procedure of conventional learning tasks. This episodic meta-training regimen is backed
23 by the assumption that a machine learning model quickly generalizes to novel unseen data with minimal
24 fine-tuning when trained and tested under similar circumstances (Vinyals et al., 2016). To facilitate such
25 a generalization capacity, a meta-training phase is undertaken, where the model is trained to optimize its
26 performance on several homogeneous tasks/episodes randomly sampled from a dataset. Each episode or task
27 is a learning problem in itself. In the few-shot setting each task is a classification problem, a collection of K
28 support (train) and Q query (test) samples corresponding to each of the N classes. Task-specific knowledge
29 is learned using the support data, and meta-knowledge across the tasks is learned using query samples,
30 which essentially encodes “how to learn a new task effectively.” The learned meta-knowledge is generic and
31 agnostic to tasks from the same distribution. It is typically characterized in two different forms - either as an
32 optimal initialization for the machine learning model or a learned parametric optimizer. Under the optimal
33 initialization view, the learned meta-knowledge represents an optimal prior over the model parameters, that
34 is equidistant, but close to the optimal parameters for all individual tasks. This enables the model to rapidly
35 adapt to unseen tasks from the same distribution (Finn et al., 2017; Li et al., 2017; Jamal & Qi, 2019).
36 Under the parametric optimizer view, meta-knowledge pertaining to the traversal of the loss surface of tasks
37 is learned by the meta-optimizer. Through learning task specific and task agnostic characteristics of the loss
38 surface, a parametric optimizer can thus effectively guide the base model to traverse the loss surface and
39 achieve superior performance on unseen tasks from the same distribution (Ravi & Larochelle, 2017).

Initialization based ML approaches accumulate the meta-knowledge by simultaneously optimizing over a batch of tasks. On the other hand, a parametric optimizer sequentially accumulates meta-knowledge across individual tasks. The sequential accumulation process leads to a long oscillatory optimization trajectory and a bias towards the last task, limiting the parametric optimizer’s task agnostic potential. However, recently meta-knowledge has been accumulated in a batch mode even for the parametric optimizer (Aimen et al., 2021). Further, under such batch episodic training (for both initialization and optimization views), a common assumption in ML that the randomly sampled episodes of a batch contribute equally to improving the learned meta-knowledge need not hold good. Due to the latent properties of the sampled tasks in a batch and the model configuration, some tasks may be better aligned with the optimal meta-knowledge than others. We hypothesize that proportioning the contribution of a task as per its alignment towards the optimal meta-knowledge can improve the meta-model’s learning. This is analogous to classical machine learning algorithms like sample re-weighting, which however, operate at sample granularity. In re-weighting, samples leading to false positives are prioritized and therefore replayed. Hence, the latent properties due to which a sample is prioritized are explicitly defined. For complex task distributions, explicitly handcrafting the notion of “importance” of a task would be hard. To this end, we propose a task attended meta-training curriculum that employs an attention module that learns to assign weights to the tasks of a batch with experience. The attention module is parametrized as a neural network that takes meta-information in terms of the model’s performance on the tasks in a batch as input and learns to associate weights to each of the tasks according to their contribution in improving the meta-model. Overall, we make the following contributions,

- We propose a task attended meta-training strategy wherein different tasks of a batch are weighted according to their “importance” defined by the attention module. This attention module is a standalone unit that can be integrated into any batch episodic training regimen.
- We extend the empirical investigation of the batch-mode parametric optimizer (MetaLSTM++) to complex datasets like miniImagenet, FC100, and tieredImageNet and validate its efficiency over its sequential counter-part (MetaLSTM).
- We conduct extensive experiments on miniImagenet, FC100, and tieredImageNet datasets and compare ML algorithms like MAML, MetaSGD, ANIL, and MetaLSTM++ with their task-attended counterparts to validate the effectiveness of the task attention module and its coupling with any batch episodic training regimen.
- We compare the proposed training curriculum with task-disagreement resolving approaches like TAML (Jamal & Qi, 2019) and conflict-averse gradient descent (Liu et al., 2021a) and validate the goodness of the proposed hypothesis. We extend these task-disagreement based approaches to the meta-learning regimen for a fair comparison.
- We further compare task-attended curriculum with state-of-the-art task scheduling approaches and also show the merit of the proposed approach on the miniImagenet-noisy dataset and cross-domain few shot learning (CDFSL) setup.
- We perform exhaustive empirical analysis and visual inspections to decipher the working of the task attention module.

2 Related Work

Transfer learning and meta-learning are two approaches that are commonly used to address few-shot learning problems. Transfer learning involves learning generalizable representations from larger datasets and models, and then using simple algorithms like fine-tuning to adapt to the specific task at hand. On the other hand, meta-learning approaches aim to find an algorithmic solution to few-shot learning. Due to their simplicity, transfer learning approaches scale well with larger image sizes and deeper models. In contrast, meta-learning approaches are memory intensive, which has become a barrier in scaling them to larger image sizes and deeper backbones (Dumoulin et al., 2021). Addressing the computational issues of meta-learning approaches and scaling them to larger support sets, deeper backbones and larger image sizes is a concurrent

area of research (Bronskill et al., 2021; Shin et al., 2021). We leave the integration of our approach with these techniques to enhance the scalability to the future. Equipped with deeper backbones and larger image sizes, transfer learning approaches achieved high performances, particularly in cross-domain settings (Bronskill et al., 2021; Guo et al., 2020; Dhillon et al., 2019; Dumoulin et al., 2021). However, a line of literature (Bronskill et al., 2021) suggests meta-learning approaches may be better suited for constrained test settings. This is because transfer learning relies on large pre-trained feature extractors and may require hundreds of optimization steps and careful hyperparameter tuning to perform well (Bronskill et al., 2021; Kolesnikov et al., 2020). For example, Meta-dataset Transfer approach (Triantafillou et al., 2019) finetunes all parameters of a ResNet18 feature backbone with a cosine classifier head for 200 optimization steps. Similarly, BiT (Kolesnikov et al., 2020) finetunes the feature backbone with a linear head, sometimes up to 20,000 optimization steps, to acquire state-of-the-art performance on VTAB dataset. Further, transfer learning approaches require significant hyper-parameter tuning on validation sets of each downstream task that also adds to the cost. On the other hand, meta-learning approaches can generalize to unseen meta-test tasks with just a few adaptation steps and often with little or no hyperparameter tuning (Bronskill et al., 2021). While transfer learning may be a better choice in some contexts, meta-learning can be a practical option in cases where computational resources are limited or when the task needs to be adapted on the fly. Overall, both approaches have their own strengths and can be useful in different settings. Our work focuses on a resource-constrained setting, where the number of support instances and the computing available for meta-test adaptation are limited. As a result, our study is confined to meta-learning setups.

ML literature is profoundly diverse and may broadly be classified into *initialization* (Finn et al., 2017; Li et al., 2017; Jamal & Qi, 2019; Raghu et al., 2020; Rusu et al., 2019; Sun et al., 2019) and *optimization approaches* (Ravi & Larochelle, 2017) depending on the metaknowledge. However, these approaches assume uniform contribution of tasks in learning a meta-model. In supervised learning, assigning non-uniform priorities to the samples is not new (Kahn & Marshall, 1953; Shrivastava et al., 2016). Self-paced learning (Kumar et al., 2010) and hard example mining (Shrivastava et al., 2016) have popularly been used to reweight the samples and various attributes like losses, gradients, and uncertainty have been used to assign priorities to samples (Lin et al., 2017; Zhao & Zhang, 2015; Chang et al., 2017). Zhao & Zhang (2015) introduce importance sampling to reduce variance and improve the convergence rate of stochastic optimization algorithms over uniform sampling. They theoretically prove that the reduction in the variance is possible if the sampling distribution depends on the norm of the gradients of the loss function. Chang et al. (2017) conclude that mini-batch SGD for classification is improved by emphasizing the uncertain examples. Lin et al. (2017) propose reshaped cross-entropy loss (focal loss) that down-weights the loss of confidently classified samples. Nevertheless, assigning non-uniform priorities to tasks in meta-learning is under-explored and has recently drawn attention (Kaddour et al., 2020; Gutierrez & Leonetti, 2020; Liu et al., 2020; Yao et al., 2021; Arnold et al., 2021). Gutierrez & Leonetti (2020) propose Information-Theoretic Task Selection (ITTS) algorithm to filter training tasks that are distinct from each other and close to the tasks of the target distribution. This algorithm results in a smaller pool of training tasks. A model trained on the smaller subset learns better than the one trained on the original set. On the other hand, Kaddour et al. (2020) propose probabilistic active meta-learning (PAML) that learns probabilistic task embeddings. Scores are assigned to these embeddings to select the next task presented to the model. These algorithms are, however, specific to meta-reinforcement learning (meta-RL). On the contrary, our focus is on the few shot classification problem. Liu et al. (2020) propose a greedy class-pair potential-based adaptive task sampling strategy wherein task selection depends on the difficulty of all class-pairs in a task. This sampling technique is static and operates at a class granularity. On the other hand, our approach is dynamic and operates at a task granularity. Assigning non-uniform weights to samples prevents overfitting on corrupt data points (Ren et al., 2018b; Jiang et al., 2018). Ren et al. (2018b) used gradient directions to re-weight the data points, and Jiang et al. (2018) learned a curriculum on examples using a mentor network. However, these approaches assume availability of abundant labeled data. Yao et al. (2021) extend Jiang et al. (2018) to the few-shot learning setup. They propose an adaptive task scheduler (ATS) to predict the sampling probability of tasks from a candidate pool containing a subset of tasks sampled from the original (noisy or imbalanced) task distribution (similar to (Jiang et al., 2018)). Thus, the sampling probabilities of the tasks are (approximately) global. Another global task sampling approach is Uniform Sampling (Arnold et al., 2021), built on the premise that task difficulty (defined as the negative log-likelihood of the model on the task) approximately follows a normal

140 distribution and is transferred across model parameters during training. They also find sampling uniformly
 141 over episode difficulty outperforms other sampling schemes like curriculum, easy and hard mining. Our
 142 work is different from these approaches (ATS and Uniform Sampling) as we do not propose a global task
 143 sampling strategy but a dynamic task-batch re-weighting mechanism for the current meta-model update.
 144 We hypothesize that the task’s importance depends on the data contained in it and the current meta-
 145 model’s configuration. For example, in the initial stage of the meta-models training, coarse-grained tasks
 146 (tasks composed of semantically distinct classes) may have higher importance than fine-grained tasks (tasks
 147 composed of comparable classes), while this behavior may reverse as the training progresses. Further,
 148 our approach differs from Uniform Sampling in the definition of task difficulty, i.e., we neither explicitly
 149 handcraft the notion of task difficulty nor assume a normal distribution over it. Instead, we let an attention
 150 network learn the suitable weights for the tasks in a batch. Although ATS also dynamically learns the task
 151 sampling priority, it maintains a candidate pool to satisfy the global task priority criteria, causing overhead.
 152 Further, it performs an additional warm start to the scheduler, utilizes more task batches in a run, and uses
 153 REINFORCE for reward estimation; therefore, it is more expensive than the proposed approach. Contrary
 154 to our idea is TAML (Jamal & Qi, 2019) - a meta-training curriculum that enforces equity across the tasks in
 155 a batch. We show that weighting the tasks according to their “importance” and hence utilizing the diversity
 156 present in a batch given the meta-model’s current configuration offers better performance than enforcing
 157 equity in a batch of tasks.

158 3 Preliminary

159 In a typical ML setting, the principal dataset \mathcal{D} is divided into disjoint meta-sets \mathcal{M} (meta-train set),
 160 \mathcal{M}_v (meta-validation set) and \mathcal{M}_t (meta-test set) for training the model, tuning its hyperparameters and
 161 evaluating its performance, respectively. Every meta-set is a collection of tasks \mathcal{T} drawn from the joint
 162 task distribution $P(\mathcal{T})$ where each task \mathcal{T}_i consists of support set $D_i = \{(x_k^c, y_k^c)_{k=1}^K\}_{c=1}^N$ and query set
 163 $D_i^* = \{(x_q^{*c}, y_q^{*c})_{q=1}^Q\}_{c=1}^N$. Here (x, y) represents a (sample, label) pair and N is the number of classes, K and
 164 Q are the number of samples belonging to each class in the support and query set, respectively. According
 165 to support-query characterization \mathcal{M} , \mathcal{M}_v and \mathcal{M}_t could be represented as $\{(D_i, D_i^*)\}_{i=1}^M$, $\{(D_i, D_i^*)\}_{i=1}^R$,
 166 $\{(D_i, D_i^*)\}_{i=1}^S$ where M , R and S are the total number of tasks in \mathcal{M} , \mathcal{M}_v and \mathcal{M}_t respectively. During
 167 meta-training, meta-model θ is adapted on D_i of all tasks in a batch $\{\mathcal{T}_i\}_{i=1}^B$ of size B , T times to obtain ϕ_i^T .
 168 The adaptation occurs through gradient descent or parametric update on the train loss L using learning rate
 169 α . The adapted model ϕ_i^T is then evaluated on D_i^* to obtain test loss L^* , which along with learning rate β ,
 170 is used to update θ . The output of this episodic training is either an optimal prior or a parametric optimizer,
 171 both aiming to facilitate the rapid adaptation of the model on unseen tasks from \mathcal{M}_t . The detailed note on
 172 initialization and optimization approaches is deferred to the supplementary material.

173 4 Task Attention in Meta-learning

174 A common assumption under the batch-wise episodic training regimen adopted by ML is that each task in a
 175 batch has an equal contribution in improving the learned meta-knowledge. However, this need not always be
 176 true. It is likely that given the current configuration of the meta-model, some tasks may be more important
 177 for the meta-model’s learning. A contributing factor to this difference is that tasks sampled from complex
 178 data distributions can be profoundly diverse. The diversity and latent properties of the tasks coupled with
 179 the model configuration may induce some tasks to be better aligned with the optimal meta-knowledge than
 180 others. The challenging aspect in the meta-learning setting is to define the “importance” and associate
 181 weights to the tasks of a batch proportional to their contribution to improving the meta-knowledge. As
 182 human beings, we *learn* to associate importance to events subjective to meta-information about the events
 183 and prior experience. This motivates us to define a learnable module that can map the meta-information of
 184 tasks to their importance weights.

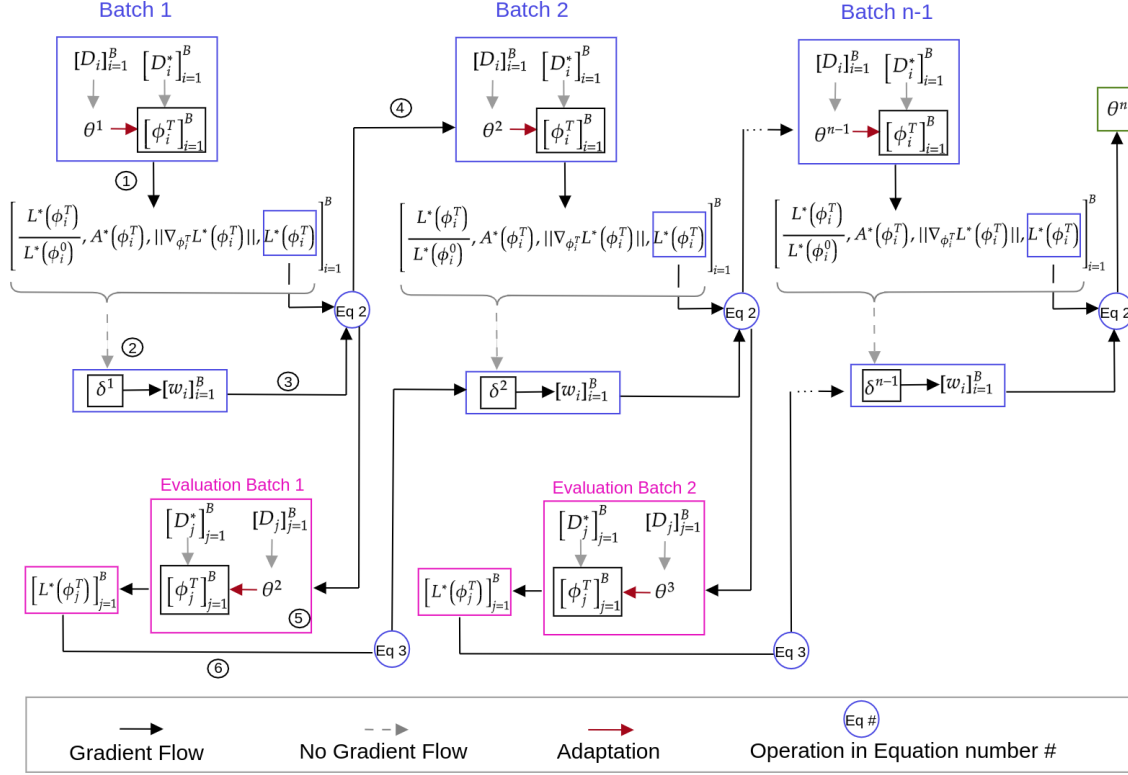


Figure 1: Computational Graph of the forward pass of the meta-model using task attended meta-training curriculum. The output of this procedure is a meta-model θ^n . Gradients are propagated through solid lines and restricted through dashed lines.

185 4.1 Characteristics of Meta-Information

186 Given a task-batch $\{\mathcal{T}_i\}_{i=1}^B$, the task attention module takes as input meta-information about each task (\mathcal{T}_i)
 187 in the batch, defined as the four tuple below:

$$\mathcal{I} = \left\{ \left(\|\nabla_{\phi_i^T} L^*(\phi_i^T)\|, L^*(\phi_i^T), A^*(\phi_i^T), \frac{L^*(\phi_i^T)}{L^*(\phi_i^0)} \right) \right\}_{i=1}^B \quad (1)$$

188 where corresponding to each task i in the batch $\|\nabla_{\phi_i^T} L^*(\phi_i^T)\|$ denotes the norm of gradient, $L^*(\phi_i^T)$ and
 189 $A^*(\phi_i^T)$ are the test loss and accuracy of the adapted model respectively, and $\frac{L^*(\phi_i^T)}{L^*(\phi_i^0)}$ is the ratio of the
 190 model's test loss post and prior adaptation.

191 4.1.1 Gradient Norm

192 Let $P = \{\phi_i^T\}_{i=1}^B$ be the parameters of the models obtained after adapting the initial model (for
 193 T iterations) on the support data $\{D_i\}_{i=1}^B$ of tasks $\{\mathcal{T}_i\}_{i=1}^B$. Also, let $G = \{\nabla_{\phi_i^T} L^*(\phi_i^T)\}_{i=1}^B$ be
 194 the gradients of the adapted model parameters w.r.t the query losses $\{L^*(\phi_i^T)\}_{i=1}^B$. The gradient
 195 norm $\{\|\nabla_{\phi_i^T} L^*(\phi_i^T)\|\}_{i=1}^B$ is the L_2 norm of the gradients and quantifies the magnitude of the con-
 196 solidified displacement of the adapted model parameters during a gradient descent update on query
 197 data. Larger gradient norm on query dataset could indicate that the model has either not learned
 198 the support set or has overfitted. Hence the model is not generalizable on query set compared to the
 199 models with low gradient norm. Gradient norm, therefore, carries information about the convergence
 200 and generalizability of the adapted models which has been theoretically studied in (Li et al., 2019).

201 **Algorithm 1:** Task Attended Meta-Training

202 **Input:**

203 *Dataset: $\mathcal{M} = \{D_i, D_i^*\}_{i=1}^M$*
 204 *Models: Meta-model θ , Base-model ϕ , Att-module δ*
 205 *Learning-rates: α, β, γ*
 206 *Parameters: Iterations n_{iter} , Batch-size B ,*
 207 *Adaptation-steps T*

208 **Output:** Meta-model θ

209 1 **Initialization:** $\theta, \delta \leftarrow$ Random Initialization

210 2 **for** iteration in n_{iter} **do**

211 3 $\{\mathcal{T}_i\}_{i=1}^B = \{D_i, D_i^*\}_{i=1}^B \leftarrow$ Sample task-batch(\mathcal{M})

212 4 **for** all \mathcal{T}_i **do**

213 5 $\phi_i^0 \leftarrow \theta$

214 6 $L^*(\phi_i^0), \dots \leftarrow evaluate(\phi_i^0, D_i^*)$ \triangleright Compute loss
and accuracy of input model on given dataset.

215 7 $\phi_i^T = adapt(\phi_i^0, D_i)$

216 8 $L^*(\phi_i^T), A^*(\phi_i^T) \leftarrow evaluate(\phi_i^T, D_i)$

217 9 **end**

218 10 $[w_i]_{i=1}^B \leftarrow Att_module$

219 11 $\left(\begin{bmatrix} L^*(\phi_i^T) \\ L^*(\phi_i^0) \end{bmatrix}, A^*(\phi_i^T), \|\nabla_{\phi_i^T} L^*(\phi_i^T)\|, L^*(\phi_i^T) \end{bmatrix}_{i=1}^B \right)$

220 12 $\theta \leftarrow \theta - \beta \nabla_\theta \sum_{i=1}^B w_i L^*(\phi_i^T)$

221 13 $\{D_j, D_j^*\}_{j=1}^B \leftarrow$ Sample task-batch(\mathcal{M})

222 14 **for** all \mathcal{T}_j **do**

223 15 $\phi_j^0 \leftarrow \theta$

224 16 $\phi_j^T = adapt(\phi_j^0, D_j)$

225 17 **end**

226 18 $\delta \leftarrow \delta - \gamma \nabla_\delta \sum_{j=1}^B L^*(\phi_j^T)$

227 19 **Return** θ

228 20 **Function** $adapt(\phi_i^t, D_i)$:

229 21 $\theta \leftarrow \phi_i^t$

230 22 **if** θ is optimal-initialization **then**

231 23 **for** $t=1$ to T **do**

232 24 $\phi_i^{t+1} \leftarrow \phi_i^t - \alpha \nabla_{\phi_i^t} L(\phi_i^t)$

233 25 **end**

234 26 **end**

235 27 **else if** θ is parametric-optimizer **then**

236 28 **for** $t=1$ to T **do**

237 29 $\phi_i^{t+1} \leftarrow \theta \left(L(\phi_i^t), \nabla_{\phi_i^t} L(\phi_i^t) \right)$ \triangleright Parameter
updates given by cell state of θ .

238 30 **end**

239 31 **end**

240 32 **Return** ϕ_i^T

241 exactly one signifies adaptation attributes to no additional benefit (neutral impact). Therefore, loss-ratio provides information regarding the impact of adaptation on each task for a given meta-model.

246 4.2 Task Attention Module

247 We learn a task attention module parameterized by δ , which attends to the tasks that contribute more to
248 the model's learning i.e., the objective of the task attention module is to learn the relative importance of

4.1.2 Test Loss

$\{L^*(\phi_i^T)\}_{i=1}^B$ represents the empirical error (cross entropy loss) of the adapted base models on unseen query instances and hence characterizes their generalizability. Unlike gradient norm, which characterizes the generalizability in parameter space, query loss quantifies generalizability in the output space as the divergence between the real and predicted probability distributions. As $\{L^*(\phi_i^T)\}_{i=1}^B$ is a key component in the meta-update equation, it is an important factor influencing the meta-model's learning. Further, test errors of classes have been widely used to determine their "easy or hardness" (Bengio et al., 2009; Liu et al., 2021b; Arnold et al., 2021). Thus $\{L^*(\phi_i^T)\}_{i=1}^B$ acquaints the attention module with the generalizability aspect of task models and their influence in updating the meta-model.

4.1.3 Test Accuracy

$\{A^*(\phi_i^T)\}_{i=1}^B$ corresponds to the accuracies of $\{\phi_i^T\}_{i=1}^B$ on $\{D_i^*\}_{i=1}^B$ scaled in the range [0,1]. $A^*(\phi_i^T)$ evaluates the thresholded predictions (predicted labels) unlike $L^*(\phi_i^T)$, which evaluates the confidence of the model's predictions on the true class labels. Two task models may predict the same class labels but differ in the confidence of the predictions. In such scenarios, neither loss nor accuracy is individually sufficient to comprehend this relationship among the tasks. So, the combination of these two entities is more reflective of the nature of the learned task models.

4.1.4 Loss-ratio

Let $L^*(\phi_i^0)$ be the loss of θ on the D_i^* , and $L^*(\phi_i^T)$ be the loss of the adapted model ϕ_i^T on D_i^* . The loss-ratio $\frac{L^*(\phi_i^T)}{L^*(\phi_i^0)}$ is representative of the relative progress of a meta-model on each task. Higher values (> 1) of the loss-ratio suggests adapting θ to D_i has an adverse effect on generalizing it to D_i^* (negative impact), while lower values (< 1) of the loss-ratio indicates the benefit of adaptation of θ on D_i (positive impact). Loss-ratio of

exactly one signifies adaptation attributes to no additional benefit (neutral impact). Therefore, loss-ratio provides information regarding the impact of adaptation on each task for a given meta-model.

249 each task in the batch for the meta-model's learning. Thus the output of the module is a B -dimensional
 250 vector $\mathbf{w} = [w_1, \dots, w_B]$, ($\sum_{i=1}^B w_i = 1$ and $\forall \mathcal{T}_i, w_i \geq 0$) quantifying the attention-score (weight - w_i) for
 251 each task. The attention vector \mathbf{w} is multiplied with the corresponding task losses of the adapted models
 252 $L^*(\phi_i^T)$ on the held-out datasets D_i^* to update the meta-model θ :

$$\theta^{t+1} \leftarrow \theta^t - \beta \nabla_{\theta^t} \sum_{i=1}^B w_i L^*(\phi_i^T) \quad (2)$$

253 After the meta-model is updated using the weighted task losses, we evaluate the goodness of the generated
 254 attention weights. We sample a new batch of tasks $\{D_j, D_j^*\}_{j=1}^B$ and adapt a base-model ϕ_j using the
 255 updated meta-model θ^{t+1} on the train data $\{D_j\}$ of each task. The mean test-loss of the adapted models
 256 $\{\phi_j^T\}_{j=1}^B$ reflect the goodness of the weights assigned by the attention-module in the previous iteration. The
 257 attention module δ is thus updated using the gradients flowing back into it w.r.t to this mean test-loss. The
 258 attention network is trained simultaneously with the meta-model in an end to end fashion using the update
 259 rule:

$$\delta^{t+1} \leftarrow \delta^t - \gamma \nabla_{\delta^t} \sum_{j=1}^B L^*(\phi_j^T) \quad (3)$$

260 where ϕ_j^T is adapted from θ^{t+1} and γ is the learning rate.

261 4.3 Task Attended Meta-Training Algorithm

262 We demonstrate the meta-training curriculum using the proposed task attention in Figure 1 and formally
 263 summarize it in Algorithm 1. [The detailed explanation is presented in Figure 7 in the appendix](#). As with
 264 the classical meta-training process, we first sample a batch of tasks from the task distribution. For each task
 265 \mathcal{T}_i , we adapt the base-model ϕ_i using the train data D_i for T time-steps (line 7 and lines 20-32 in Algorithm
 266 1). Specifically, for initialization approaches, adaptation is performed by gradient descent on train loss L
 267 (lines 22-26 in Algorithm 1). However, for optimization approaches, current loss and gradients are inputted
 268 to the meta-model θ , which outputs the updated base-model parameters (lines 27-31 in Algorithm 1). Then
 269 we compute the meta-information about the adapted model corresponding to each task. It comprises of
 270 the loss $L^*(\phi_i^T)$, accuracy $A^*(\phi_i^T)$, loss-ratio $\frac{L^*(\phi_i^T)}{L^*(\phi_i^0)}$ and gradient norm $\|\nabla_{\phi_i^T} L^*(\phi_i^T)\|$ on the test data D_i^* .
 271 This meta-information corresponding to each task in a batch is given as input to the task attention module
 272 (Figure 1 - Label: ②) which outputs the attention vector (line 10 in Algorithm 1). The attention vector
 273 and test losses $\{L^*(\phi_i^T)\}_{i=1}^B$ are used to update meta-model parameters θ according to equation 2 (line 11 in
 274 Algorithm 1, Figure 1 - Label: ④). We sample a new batch of tasks $\{D_j, D_j^*\}_{j=1}^B$ and adapt the base-models
 275 $\{\phi_j^T\}_{j=1}^B$ using the updated meta-model (lines 12-16 in Algorithm 1, Figure 1 - Label: ⑤). We compute the
 276 mean test loss over the adapted base-models $\{L^*(\phi_j^T)\}_{j=1}^B$, which is then used to update the parameters of
 277 the task attention module δ according to equation 3 (line 17 in Algorithm 1, Figure 1 - Label: ⑥).

The attention network is designed as a stand-alone module to learn the mapping from the meta-information space to the importance of tasks in a batch. The meta-model is learned according to equation 2 and aims to minimize the weighted loss. It is important to decouple the learning of the attention network from that of the meta-model. If there is information flow from the task attention module to the meta-model, the latter may reduce its weighted loss by learning an initialization that is suboptimal, but for which the task attention network assigns lower weights. This would introduce an undesirable bias to the learning process. To circumvent this bias, we restrict the flow of gradients to the meta-model θ through the task attention module δ by enforcing $\nabla_{\theta} w_i L^*(\phi_i^T) = w_i \nabla_{\theta} L^*(\phi_i^T)$ i.e., $\nabla_{\theta} w_i$ is not computed. Also, gradients flowing through the attention network to the meta-model create additional computational overhead. Specifically, the term $\nabla_{\theta} \sum_i w_i L^*(\phi_i^T)$ from equation 2 can be expanded as follows -

$$\nabla_{\theta} \sum_i w_i L^*(\phi_i^T) = \sum_i \underbrace{\nabla_{\theta} w_i L^*(\phi_i^T)}_{\text{Term 1}} + \underbrace{\sum_i w_i \nabla_{\theta} L^*(\phi_i^T)}_{\text{Term 2}} + \sum_i L^*(\phi_i^T) \nabla_{\theta} w_i$$

278 The $\nabla_\theta w_i$ in Term 2 is computationally expensive as $\nabla_\theta w_i = \nabla_\delta w_i \cdot \nabla_I \delta \cdot \nabla_\phi I \cdot \nabla_\theta \phi$. Restricting the gradient
 279 flow avoids these additional computations. We also note that the meta-model and attention network are
 280 updated only once during each training iteration, although on different batches of tasks.

281 5 Experiments and Results

282 We conduct experiments to demonstrate the merit of the task-attention across multiple datasets, training
 283 setups, and learning paradigms. We verify that the proposed regimen could be integrated with various
 284 ML approaches like MAML, MetaSGD, MetaLSTM++, and ANIL and further show its superiority over
 285 state-of-the-art task-scheduling and conflict-resolving approaches. We also analyze the attention network.

286 5.1 Dataset and Implementation Details

287 In line with the state-of-the-art literature (Sun et al.,
 288 2020; Arnold et al., 2021), we use miniImagenet, FC100,
 289 and tieredImageNet for evaluating the effectiveness of the
 290 proposed attention module as they are more challenging
 291 datasets comprising of highly diverse tasks. We also test
 292 the efficacy of the proposed approach on noisy dataset
 293 (miniImagenet-noisy), and under cross-domain few shot
 294 learning (CFSFL) miniImagenet \rightarrow CUB-200 and mini-
 295 Imagenet \rightarrow FGVC-Aircrafts datasets. The details of the
 296 datasets are presented in the supplementary material.

297 We use a 4-layer CNN from (Finn et al., 2017) as a base
 298 model and a two-layer LSTM (Ravi & Larochelle, 2017)
 299 for the parametric optimizer. The architecture of the
 300 task-attention module is illustrated in Figure 2 and de-
 301 scribed as follows. The task attention module is implemented as a 4-layer neural network. The first layer
 302 performs a 1×1 convolution over the input (meta-information) of size $B \times 4$ where B denotes the meta-batch
 303 size, producing a vector of size $B \times 1$ as output. This vector is then passed through two fully connected
 304 layers with 32 hidden nodes, each followed by a ReLU activation. This output is then passed through a fully
 305 connected layer with B nodes, followed by a softmax activation to produce the normalized attention weights.

306 We perform a grid search over
 307 30 different configurations for
 308 5000 iterations to find the optimal
 309 hyper-parameters for each setting.
 310 The search space is shared across all meta-training
 311 algorithms and datasets. The meta, base and attention model
 312 learning rates are sampled
 313 from a log uniform distribution
 314 in the ranges $[1e^{-4}, 1e^{-2}]$,
 315 $[1e^{-2}, 5e^{-1}]$ and $[1e^{-4}, 1e^{-2}]$
 316 respectively (see appendix for
 317 more details). The hyperpara-
 318 meter λ for TAML (Theil)
 319 is sampled from a log uniform
 320 distribution over the range of
 321 $[1e^{-2}, 1]$. For CA-MAML, c is
 322 set as 0.5. The meta-batch size
 323 is set to 4 for all settings (Finn
 324 et al., 2017; Jamal & Qi, 2019).

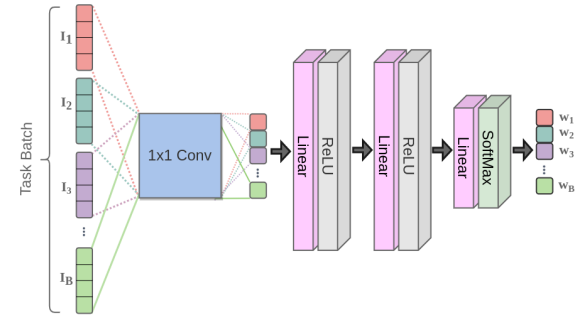


Figure 2: Architecture of Task-attention module.

Table 1: Comparison of few-shot classification performance of MAML and TA-MAML on miniImagenet dataset with meta-batch size 4 and 6 and 8 for 5 and 10 way (1 and 5 shot) settings. The \pm represents the 95% confidence intervals over 300 tasks. Algorithms denoted by * are rerun on their optimal hyper-parameters on our experimental setup. We observe that TA-MAML consistently performs better than MAML, and an increase in the tasks in a batch improves the performance of both MAML and TA-MAML.

| Model | Test Accuracy (%) on miniImagenet | | | |
|--------------|-------------------------------------|-------------------------------------|-------------------------------------|------------------------------------|
| | 5 Way | | 10 Way | |
| | 1 Shot | 5 Shot | 1 Shot | 5 Shot |
| Batch Size 4 | | | | |
| MAML* | 46.10 \pm 0.19 | 60.16 \pm 0.17 | 29.42 \pm 0.11 | 41.98 \pm 0.10 |
| TA-MAML* | 48.36 \pm 0.23 | 62.48 \pm 0.18 | 31.15 \pm 0.11 | 43.70 \pm 0.09 |
| Batch Size 6 | | | | |
| MAML* | 47.72 \pm 1.041 | 63.45 \pm 1.083 | 31.55 \pm 0.626 | 46.27 \pm 0.64 |
| TA-MAML* | 49.14 \pm 1.211 | 65.26 \pm 0.956 | 32.62 \pm 0.635 | 46.67 \pm 0.63 |
| Batch Size 8 | | | | |
| MAML* | 47.68 \pm 1.20 | 63.81 \pm 0.98 | 31.54 \pm 0.66 | 46.15 \pm 0.58 |
| TA-MAML* | 50.35 \pm 1.22 | 65.69 \pm 1.08 | 32.00 \pm 0.68 | 48.33 \pm 0.63 |

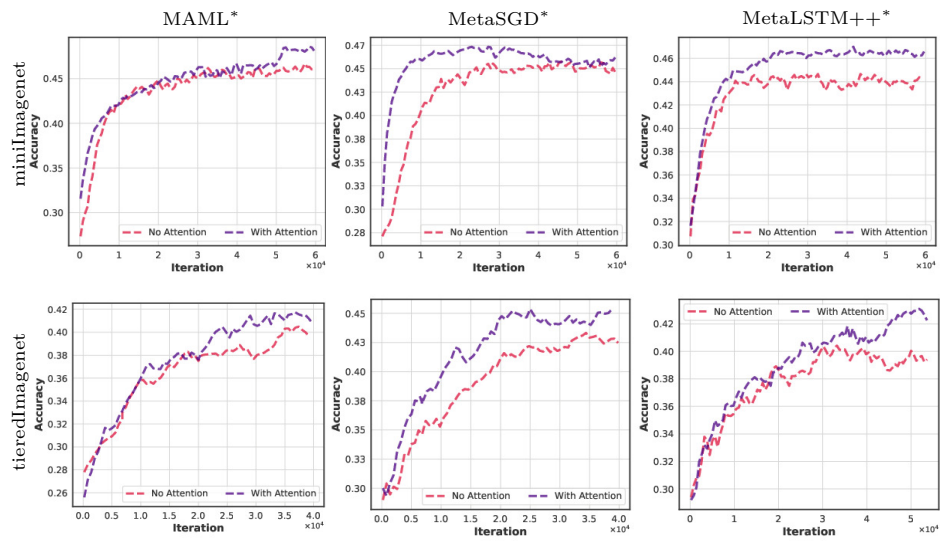
327 However, we study its impact in Table 1. All models were trained for 55000 iterations (early stopping was
 328 employed for tieredImageNet) using the optimal set of hyper-parameters using an Adam optimizer (Kingma
 329 & Ba, 2015). All the experimental results and comparisons correspond to our re-implementation of the ML
 330 algorithms integrated into learn2learn library (Arnold et al., 2020) to ensure fairness and uniformity. We
 331 believe that integrating the proposed attention module and additional ML algorithms into the learn2learn
 332 library will benefit the ML community. We perform individual hyperparameter tuning for all the models
 333 over the same hyperparameter space to ensure a fair comparison. The source code is publicly available.¹

334 The literature reports significant variations in the meta-test performances of various ML approaches (Table
 335 7 in supplementary material). The reported average meta-test accuracies of MAML on the miniImagenet
 336 dataset range from 46.47 % to 48.70 % (55.16% to 64.39%) for 5 way 1 shot (5 shot) settings. A careful
 337 analysis reveals the different experimental setups resulting in the observed variation. Experimental setups
 338 (Finn et al., 2017; Oreshkin et al., 2018; Oh et al., 2020) differ in the number of examples per class in the
 339 query set, the number of gradient descent steps in the inner loop, meta-batch size, inductive or transductive
 340 batch normalization, etc. We conduct two sets of experiments to test the proposed task attention model’s
 341 efficacy in a fair manner. The first set of experiments use the train and test setups reported in the literature
 342 (denoted using #). The second set uses our setup (denoted using *) that has the same train and test
 343 conditions. Specifically, we set the query examples per class to 15 and gradient steps to 5 for both the meta-
 344 train and meta-test phases. However, for 10 way 5 shot setting, we use only 2 gradient steps to reduce the
 345 computational burden. More query examples per class (15) during the meta-test provide a robust estimate of
 346 the model’s generalizability. Further, setting gradient steps to 5 (or 2) better evaluates the quick adaptation
 347 capabilities of a learned prior.

348 5.2 Influence of Task Attention on Meta-Training

349 As task-attention (TA) is a standalone module, it can be integrated with any batch episodic training reg-
 350 imen. We, therefore, use MetaLSTM++ (batch mode of MetaLSTM) for our experiments. In (Aimen
 351 et al., 2021), authors demonstrated the merit of MetaLSTM++ on MetaLSTM only on Omniglot dataset.
 352 We extend upon this empirical investigation by comparing the performance of MetaLSTM and MetaL-
 353 STM++ on complex datasets like miniImagenet, FC100, and tieredImageNet (Table 2). It is evident
 354 from the results that batch-wise episodic training is more effective than sequential episodic training.

355 We also investigate the
 356 performance of models
 357 trained with the TA
 358 meta-training regimen
 359 with their non-TA coun-
 360 terparts on both (our
 361 and reported - where-
 362 ever available) setups.
 363 Specifically, we compare
 364 MAML, MetaSGD,
 365 MetaLSTM++, and
 366 ANIL with their task-
 367 attended versions on 5
 368 and 10 way (1 and 5
 369 shot) settings on mini-
 370 Imagenet, FC100, and
 371 tieredImageNet datasets
 372 and report the results
 373 in Table 2. We consider
 374 300 meta-test tasks for
 375 all approaches unless
 376 specified otherwise. For



377 Figure 3: Mean validation accuracies of MAML* (Col-1), MetaSGD* (Col-2) and
 378 MetaLSTM++* (Col-3) across 300 tasks with/without attention on 5 way 1 shot
 379 setting on miniImagenet (Row-1) and tieredImageNet (Row-2) datasets.

¹<https://github.com/taskattention/task-attended-metalearning.git>

Table 2: Comparison of few-shot classification performance of vanilla ML algorithms with their task attended versions on miniImagenet, FC100 and tieredImageNet datasets for 5 and 10 way (1 and 5 shot) settings. The \pm represents the 95% confidence intervals over 300 tasks. Algorithms denoted by * and # are rerun on using the optimal hyper-parameters on our and reported experimental setups, respectively. Attention-based ML algorithms perform better than their corresponding vanilla approaches across all the settings. Further, MetaLSTM++ and TA-MAML perform better than MetaLSTM and TAML (and CA-MAML), respectively, across all settings and datasets.

| Model | Test Accuracy (%) | | | |
|------------------------------|------------------------------------|------------------------------------|------------------------------------|------------------------------------|
| | 5 Way | | 10 Way | |
| | 1 Shot | 5 Shot | 1 Shot | 5 Shot |
| miniImagenet | | | | |
| MAML# (Finn et al., 2017) | 48.07 \pm 1.75 | 63.15 \pm 0.91 | - | - |
| CA-MAML# (Liu et al., 2021a) | 47.86 \pm 2.50 | 64.27 \pm 1.26 | - | - |
| TAML# (Jamal & Qi, 2019) | 51.77 \pm 1.86 | 65.6 \pm 0.93 | - | - |
| TA-MAML# | 53.80 \pm 1.85 | 66.11 \pm 0.11 | - | - |
| MetaSGD* | 46.10 \pm 0.19 | 60.16 \pm 0.17 | 29.42 \pm 0.11 | 41.98 \pm 0.10 |
| TAML* | 46.26 \pm 0.21 | 53.40 \pm 0.14 | 29.76 \pm 0.11 | 36.88 \pm 0.10 |
| TA-MAML* | 48.36 \pm 0.23 | 62.48 \pm 0.18 | 31.15 \pm 0.11 | 43.70 \pm 0.09 |
| MetaSGD# (Li et al., 2017) | 50.47 \pm 1.87 | 64.03 \pm 0.94 | - | - |
| TA-MetaSGD# | 52.60 \pm 0.25 | 67.54 \pm 0.12 | - | - |
| MetaSGD* | 47.65 \pm 0.21 | 61.60 \pm 0.17 | 30.09 \pm 0.10 | 42.22 \pm 0.11 |
| TA-MetaSGD* | 49.28 \pm 0.20 | 63.37 \pm 0.16 | 31.50 \pm 0.11 | 44.06 \pm 0.10 |
| MetaLSTM* | 41.48 \pm 1.02 | 58.87 \pm 0.94 | 28.62 \pm 0.64 | 44.03 \pm 0.69 |
| MetaLSTM++* | 48.00 \pm 0.19 | 62.73 \pm 0.17 | 31.16 \pm 0.09 | 45.46 \pm 0.10 |
| TA-MetaLSTM++* | 49.18 \pm 0.17 | 64.89 \pm 0.16 | 32.07 \pm 0.11 | 46.66 \pm 0.09 |
| ANIL# (Raghu et al., 2020) | 46.7 \pm 0.4 | 61.5 \pm 0.5 | - | - |
| TA-ANIL# | 49.53 \pm 0.41 | 63.73 \pm 0.33 | - | - |
| ANIL* | 46.92 \pm 0.62 | 58.68 \pm 0.54 | 28.84 \pm 0.34 | 40.95 \pm 0.32 |
| TA-ANIL* | 48.84 \pm 0.62 | 60.80 \pm 0.55 | 31.14 \pm 0.34 | 42.52 \pm 0.34 |
| FC100 | | | | |
| MAML* | 36.40 \pm 0.38 | 46.76 \pm 0.21 | 23.93 \pm 0.14 | 31.14 \pm 0.07 |
| TAML* | 38.00 \pm 0.26 | 48.05 \pm 0.13 | 21.60 \pm 0.14 | 33.19 \pm 0.07 |
| TA-MAML* | 39.86 \pm 0.25 | 49.56 \pm 0.13 | 25.46 \pm 0.15 | 36.06 \pm 0.08 |
| MetaSGD* | 33.46 \pm 0.23 | 43.96 \pm 0.13 | 21.40 \pm 0.15 | 30.59 \pm 0.07 |
| TA-MetaSGD* | 35.66 \pm 0.25 | 49.49 \pm 0.12 | 23.80 \pm 0.15 | 32.08 \pm 0.07 |
| MetaLSTM* | 37.20 \pm 0.26 | 47.89 \pm 0.13 | 21.70 \pm 0.14 | 32.11 \pm 0.07 |
| MetaLSTM++* | 38.60 \pm 0.23 | 49.82 \pm 0.12 | 22.80 \pm 0.14 | 33.46 \pm 0.08 |
| TA-MetaLSTM++* | 41.53 \pm 0.28 | 51.17 \pm 0.13 | 25.33 \pm 0.15 | 34.18 \pm 0.08 |
| ANIL* | 34.08 \pm 1.29 | 44.74 \pm 0.68 | 20.65 \pm 0.77 | 27.93 \pm 0.42 |
| TA-ANIL* | 38.06 \pm 1.26 | 46.94 \pm 0.69 | 23.27 \pm 0.79 | 28.29 \pm 0.40 |
| tieredImageNet | | | | |
| MAML# (Oh et al., 2020) | 47.44 \pm 0.18 | 64.70 \pm 0.14 | - | - |
| TA-MAML# | 51.90 \pm 0.19 | 69.43 \pm 0.18 | - | - |
| MAML* | 44.40 \pm 0.49 | 57.07 \pm 0.22 | 27.40 \pm 0.25 | 34.30 \pm 0.14 |
| TAML* | 46.40 \pm 0.40 | 56.80 \pm 0.23 | 26.40 \pm 0.25 | 34.40 \pm 0.15 |
| TA-MAML* | 48.40 \pm 0.46 | 60.40 \pm 0.25 | 31.00 \pm 0.26 | 37.60 \pm 0.15 |
| MetaSGD* | 52.80 \pm 0.44 | 62.35 \pm 0.26 | 31.90 \pm 0.27 | 44.16 \pm 0.15 |
| TA-MetaSGD* | 56.20 \pm 0.45 | 64.56 \pm 0.24 | 33.20 \pm 0.29 | 47.12 \pm 0.16 |
| MetaLSTM* | 37.00 \pm 0.44 | 59.83 \pm 0.25 | 29.80 \pm 0.28 | 39.28 \pm 0.13 |
| MetaLSTM++* | 47.60 \pm 0.49 | 63.24 \pm 0.25 | 30.70 \pm 0.27 | 47.97 \pm 0.16 |
| TA-MetaLSTM++* | 49.00 \pm 0.44 | 66.15 \pm 0.23 | 32.10 \pm 0.27 | 51.35 \pm 0.17 |
| ANIL* | 45.08 \pm 1.37 | 59.71 \pm 0.77 | 29.32 \pm 0.83 | 42.76 \pm 0.50 |
| TA-ANIL* | 45.96 \pm 1.32 | 60.96 \pm 0.72 | 32.68 \pm 0.92 | 47.56 \pm 0.51 |

377 ANIL and its task-attended counterpart, we consider 1000 testing tasks. From Table 2, we observe that
 378 models trained with TA regimen generalize better to the unseen meta-test tasks than their non-task-attended
 379 versions across all the settings in all datasets. Note that the proposed task attention mechanism aims not
 380 to surpass the state-of-the-art meta-learning algorithms but provides new insight into the batch episodic
 381 meta-training regimen, which as per our knowledge, is common to all meta-learning algorithms.

382 We also compare the performance of TA-MAML against TAML - a meta-training regimen that forces the
 383 meta-model to be equally close to all the tasks. The results, as presented in Table 2, suggest that TA-MAML
 384 performs better than TAML on all benchmarks across all settings. Note that both TAML and TA-MAML
 385 are approaches that built upon MAML to address the inequality/diversity of tasks in a batch. Our aim is
 386 thus to compare TAML and TA-MAML and not to assess the efficacy of TAML when meta-trained using
 387 task attention. Liu et al. (2021a) proposed an optimization method to neutralize conflicts of an average
 388 model with individual tasks in a multi-task learning setup. Specifically, they find an optimal update vector
 389 that lies in the proximity of the average gradient across the batch of the tasks without conflicting with any
 390 task gradient. This method is similar to (Jamal & Qi, 2019) in a meta-learning setup, which constrains
 391 the losses of tasks towards the average loss on a task batch. As the update vector is constrained to be
 392 close to the average gradient vector on a task batch, information flow from certain useful tasks to the meta-
 393 model may decrease. We note that we extend (Liu et al., 2021a) to a meta-learning setup by computing
 394 the average and weighted average gradients on query loss of the adapted models instead of a model from
 395 the previous iteration (as in a multi-task setup). Table 2 demonstrates that the proposed attention mech-
 396 anism has better generalizability to unseen tasks than conflict-averse gradient descent adapted for a meta-
 397 learning setup (CA-MAML). Our approach utilizes a non-linear model to extract knowledge from multiple
 398 meta-information components to learn the weights, which helps it to outperform TAML and CA-MAML.
 399

400 We investigate the influence of the TA meta-
 401 training regimen on the model’s convergence by
 402 analyzing the trend of the model’s validation ac-
 403 curacy over iterations. Figure 3 depicts the mean
 404 validation accuracy over 300 tasks on miniImagenet
 405 and tieredImageNet datasets for a 5 way 1 shot set-
 406 ting across training iterations. We observe that
 407 the models meta-trained with TA regimen tend to
 408 achieve higher/at-par performance in fewer iter-
 409 ations than the corresponding models meta-trained
 410 with the non-TA regimen.

411 5.3 Comparison with Sampling Approaches

412 We compare our proposed approach with ATS (Yao
 413 et al., 2021) and uniform sampling (Arnold et al.,
 414 2021) and demonstrate that our weighting mecha-
 415 nism imparts better generalizability to the meta-
 416 model than the global weighting of the tasks.

417 Yao et al. (2021) ascertained the merit of ATS
 418 over Greedy class-pair (GCP) technique (Liu et al.,
 419 2020) on miniImagenet dataset. We extend this
 420 comparison and show in Table 3 that the pro-
 421 posed approach performs better than state-of-the-
 422 art ATS and GCP in both 1 and 5 shot settings.
 423 We also observe that the TA mechanism performs
 424 better than uniform sampling on the miniImagenet
 425 dataset on 1 and 5 shot settings for MAML and
 426 ANIL. ATS has been designed for noisy and im-
 427 balanced task distributions. So, we compare the

Table 3: Comparison (Test Accuracy (%)) of task attention with GCP, ATS and Uniform Sampling for MAML and MetaSGD (or ANIL) on miniImagenet dataset and various sampling techniques for ANIL on the miniImagenet-noisy dataset for 5 way 1 and 5 shot settings. For miniImagenet, algorithms denoted by * and # are rerun on the optimal hyper-parameters on our and reported experimental setups, respectively.

| Model | 5 Way | |
|-------------------------------------|---------------------|---------------------|
| | 1 Shot | 5 Shot |
| miniImagenet | | |
| MAML with GCP# | 46.92 ± 0.83 | 63.28 ± 0.66 |
| MAML with ATS# | 47.89 ± 0.77 | 64.07 ± 0.70 |
| MAML+UNIFORM (Offline) [#] | 46.67 ± 0.63 | 62.09 ± 0.55 |
| MAML+UNIFORM (Online) [#] | 46.70 ± 0.61 | 61.62 ± 0.54 |
| TA-MAML* (Ours) | 48.36 ± 0.23 | 62.48 ± 0.18 |
| TA-MAML# (Ours) | 53.80 ± 1.85 | 66.11 ± 0.11 |
| MetaSGD with GCP# | 47.77 ± 0.75 | 63.50 ± 0.71 |
| MetaSGD with ATS# | 48.59 ± 0.79 | 64.79 ± 0.74 |
| TA-MetaSGD* (Ours) | 49.28 ± 0.20 | 63.37 ± 0.16 |
| TA-MetaSGD# (Ours) | 52.60 ± 0.25 | 67.54 ± 0.12 |
| ANIL+UNIFORM (Offline) [#] | 46.93 ± 0.62 | 62.75 ± 0.60 |
| ANIL+UNIFORM (Online) [#] | 46.82 ± 0.63 | 62.63 ± 0.59 |
| TA-ANIL* (Ours) | 48.84 ± 0.62 | 60.80 ± 0.55 |
| TA-ANIL# (Ours) | 49.53 ± 0.41 | 63.73 ± 0.33 |
| miniImagenet-noisy | | |
| Uniform | 41.67 ± 0.80 | 55.80 ± 0.71 |
| SPL | 42.13 ± 0.79 | 56.19 ± 0.70 |
| Focal Loss | 41.91 ± 0.78 | 53.58 ± 0.75 |
| GCP | 41.86 ± 0.75 | 54.63 ± 0.72 |
| PAML | 41.49 ± 0.74 | 52.45 ± 0.69 |
| DAML | 41.26 ± 0.73 | 55.46 ± 0.70 |
| ATS | 44.21 ± 0.76 | 59.50 ± 0.71 |
| TA-ANIL* (Ours) | 45.17 ± 0.23 | 62.15 ± 1.01 |

proposed approach with GCP, ATS, and other sampling techniques on the miniImagenet-noisy dataset (Yao et al., 2021) and report the results in Table 3. We observe that task attention outperforms all scheduling algorithms on the miniImagenet-noisy dataset. As ATS is the most competitive baseline for the proposed method on the miniImagenet-noisy dataset, we compare the TA-ANIL and ATS on varying noise ratios for the miniImagenet dataset on 5 way 1 shot setting (Table 4). We observe that the proposed method outperforms ATS on all noise ratios except 0.8. Note that the algorithm used for all sampling approaches is ANIL.

5.4 Effectiveness of Task Attention in CDFSL setup

Classical meta-learning approaches assume meta-train and meta-test data belong to the same distribution such that the meta-trained model extends its knowledge to the meta-test set. This is, however, not always the case. The difference in the data acquisition techniques, or evolution

of data with time, may cause a discrepancy between the meta-train and meta-test distributions. This realistic setting is popularly termed as cross-domain few-shot learning (CDFSL) (Guo et al., 2020). We conducted experiments to show the merit of the proposed approach in CDFSL setup. Specifically, we train a model using a TA meta-training regimen on the miniImagenet dataset and meta-test it on CUB-200, FGVC-Aircraft, Describable Textures, and Omniglot datasets from Metadataset (Triantafillou et al., 2019). The results reported for 5 way 1 and 5 shot settings in Table 5 indicate that the proposed approach outperforms the state-of-the-art task scheduling approach (Uniform Sampling - wherever applicable) or non-task-attended counterparts (for Omniglot) on CDFSL setup by a large margin.

As some classes of Imagenet overlap with Metadataset, we also conduct experiments on the diverse VTAB dataset (Zhai et al., 2019), which does not share classes with the Imagenet (consequently miniImagenet) dataset. We note that some VTAB sub-datasets like Sun397 are quite memory intensive and others like Patch Camelyon, Retinopathy, etc., have fewer classes. In the interest of time and resources, we meta-train a conv4 model on the miniImagenet dataset and evaluate it on a few of feasible sub-datasets covering all three domains - Natural, Specialized, and Structured. Specif-

Table 4: Comparative analysis of ANIL integrated with ATS and proposed method on miniImagenet dataset with varying noise ratios for 5 way 1 shot setting. BNS is the best non-adaptive scheduler.

| Noise ratio | Test Accuracy (%) on miniImagenet-noisy | | | |
|------------------------|---|---------------------|---------------------|---------------------|
| | 0.2 | 0.4 | 0.6 | 0.8 |
| ANIL with Uniform | 43.46 ± 0.82 | 42.92 ± 0.78 | 41.67 ± 0.80 | 36.53 ± 0.73 |
| ANIL with BNS | 44.04 ± 0.81 | 43.36 ± 0.75 | 42.13 ± 0.79 | 38.21 ± 0.75 |
| ANIL with ATS | 45.55 ± 0.80 | 44.50 ± 0.86 | 44.21 ± 0.76 | 42.18 ± 0.73 |
| TA-ANIL* (Ours) | 47.98 ± 0.26 | 46.69 ± 0.22 | 45.17 ± 0.23 | 40.35 ± 1.14 |

Table 5: Comparative analysis of proposed approach (TA-MAML) and uniform sampling (Arnold et al., 2021) (or non-task attended counterpart (MAML)) in a CDFSL setting after training on miniImagenet dataset and tested on Metadataset and VTAB datasets for 5 way 1 and 5 shot settings.

| Model | 5 Way | | 5 Way | |
|-------------------------------------|---------------------|---------------------|---------------------|---------------------|
| | 1 Shot | 5 Shot | 1 Shot | 5 Shot |
| Metadataset | | | | |
| CUB-200 | | | | |
| MAML+ UNIFORM (Online) [#] | 35.84 ± 0.54 | 46.67 ± 0.55 | 26.62 ± 0.39 | 34.41 ± 0.44 |
| TA-MAML[#] (Ours) | 42.87 ± 1.18 | 57.49 ± 0.99 | 29.42 ± 0.78 | 36.34 ± 0.86 |
| Describable Textures | | | | |
| MAML+ UNIFORM (Online) [#] | 31.84 ± 0.49 | 40.81 ± 0.44 | | |
| TA-MAML[#] (Ours) | 31.98 ± 0.98 | 44.39 ± 0.79 | | |
| Omniglot | | | | |
| MAML [#] | 72.40 ± 1.43 | 86.81 ± 0.99 | | |
| TA-MAML[#] (Ours) | 78.73 ± 1.08 | 88.92 ± 0.76 | | |
| VTAB Dataset | | | | |
| FC100 | | | | |
| MAML [#] | 35.49 ± 1.95 | 44.42 ± 0.83 | 51.93 ± 1.59 | 75.22 ± 0.48 |
| TA-MAML[#] (Ours) | 38.87 ± 1.90 | 46.57 ± 0.85 | 61.86 ± 1.72 | 77.49 ± 0.16 |
| SVHN | | | | |
| MAML [#] | 20.93 ± 1.01 | 22.42 ± 0.88 | | |
| TA-MAML[#] (Ours) | 21.73 ± 1.09 | 24.20 ± 0.78 | | |
| EuroSAT | | | | |
| MAML [#] | 45.80 ± 1.49 | 62.0 ± 0.71 | 33.60 ± 1.49 | 42.07 ± 0.37 |
| TA-MAML[#] (Ours) | 51.67 ± 1.62 | 66.69 ± 0.70 | 35.20 ± 1.21 | 46.27 ± 0.39 |
| DSprites_location | | | | |
| MAML [#] | 36.67 ± 1.55 | 48.91 ± 0.84 | 20.86 ± 1.81 | 22.89 ± 0.95 |
| TA-MAML[#] (Ours) | 39.93 ± 1.33 | 56.48 ± 0.95 | 24.27 ± 1.18 | 22.92 ± 0.93 |
| DSprites_orientation | | | | |

480 ically, we investigate the merit of the proposed approach on Natural sub-datasets like DTD, CIFAR FC 100,
 481 Flowers102, and SVHN, specialized sub-datasets like EuroSAT and Resisc45, and structured sub-datasets like
 482 dSprites_location and dSprites_orientation. We have kept Describable Textures as a part of Metadataset
 483 and Flowers102 as a component of VTAB dataset according to (Dumoulin et al., 2021). We convert the se-
 484 lected VTAB sub-datasets to a few-shot setup (5-way 1 and 5 shot tasks) and evaluate task-attended MAML
 485 (TA-MAML) and its vanilla version (MAML) on 300 tasks. Our experiments (Table 5) demonstrate that task
 486 attention allows MAML to better generalize to unseen, diverse out-of-distribution VTAB meta-test sets.

487 5.5 Ablation Studies

488 To examine the significance of each input
 489 given to the task attention model, we con-
 490 duct an ablation study on 5 way 1 and 5 shot
 491 TA-MAML on miniImagenet dataset and
 492 report the results in Table 6. We observe
 493 that all the components of meta-information
 494 contribute to the learning of a more general-
 495 izable meta-model. To further support this
 496 observation, we investigate the relationship
 497 between the meta-information and weights
 498 assigned by the task attention module by
 499 analyzing the mean Pearson correlation of
 500 each of the components (four tuple) of the meta-information with the attention vector across the training
 501 iterations. This is depicted in Figure 4 for TA-MAML on 5 way 1 and 5 shot settings for miniImagenet
 502 dataset. We observe that the loss ratio and loss are positively correlated with the attention vector, while
 503 accuracy and gradient norm are negatively correlated.

504 In 5 way 5 shot setting, we observe that the correlation pattern is comparable to 5 way 1 shot setting, but
 505 the mean correlation value of grad norm across iterations is less than that of the 5 way 1 shot setting. This
 506 could be because the 5 way 5 shot setting is richer in data than the 5 way 1 shot setting, which allows better
 507 learning and therefore has low average values of grad norm (Section 4.1.1). The critical observation, however,
 508 is that the meta-information components have a weak correlation with the attention weights, indicating that
 509 the TA module does not trivially follow any single component of meta-information. We also analyze the
 510 ranks of the tasks for maximum and minimum values of : loss, loss ratio, accuracy, and grad norm in a
 511 batch, as per the weights across training iterations, and describe results in the supplementary material. The
 512 rank analysis also reinforces the same observation. We ascertain the decreasing trend of mean weighted loss
 513 across iterations in the supplementary material.

514 5.6 Analysis of Attention Network

515 To gain further insights into the op-
 516 eration of the attention module, we
 517 also examine the trend of the attention-
 518 vector (Figure 5) while meta-training
 519 TA-MAML for 5 way 1 and 5 shot set-
 520 tings on the miniImagenet dataset. We
 521 plot the maximum and the minimum at-
 522 tention score assigned to the tasks of a
 523 batch across iterations together with a
 524 few weighted task batches in 5 way 1 shot
 525 setting for illustration. We note that the
 526 weighted task batches are only intended
 527 to demonstrate the change in the tasks’
 528 attention scores across iterations. The next experiment presents

Table 6: Effect of ablating components of meta-information in TA-MAML* for 5 way 1 and 5 shot settings on miniImagenet dataset.

| Grad norm | Loss | Loss-ratio | Accuracy | Ablation on inputs | |
|-----------|------|------------|----------|--------------------|-------------------|
| | | | | 5 way 1 shot | 5 way 5 shot |
| ✗ | ✗ | ✗ | ✗ | 46.10±0.19 | 60.16±0.17 |
| ✓ | ✓ | ✓ | ✗ | 47.30±0.16 | 60.48±0.16 |
| ✓ | ✓ | ✗ | ✓ | 47.62±0.17 | 62.17±0.17 |
| ✓ | ✗ | ✓ | ✓ | 48.10±0.18 | 60.90±0.20 |
| ✗ | ✓ | ✓ | ✓ | 47.30±0.18 | 61.52±0.16 |
| ✓ | ✓ | ✓ | ✓ | 48.36±0.23 | 62.48±0.18 |

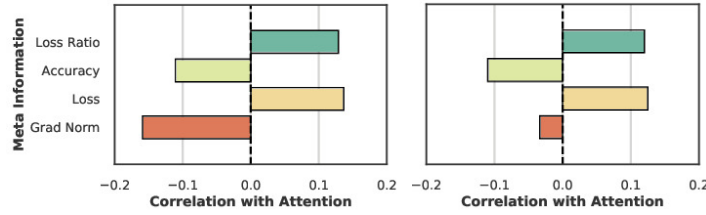
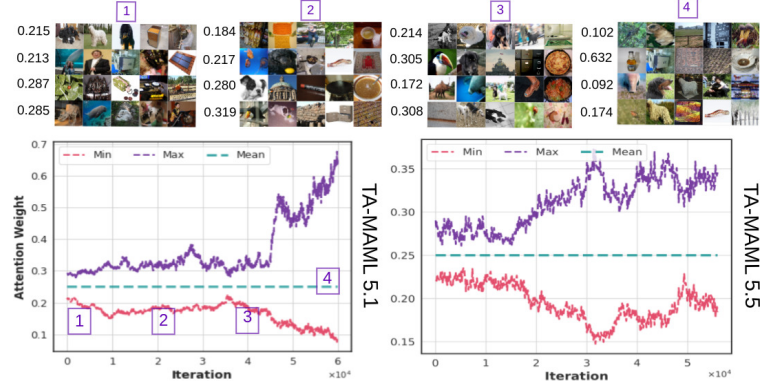


Figure 4: Mean Pearson correlation of TA-MAML* on 5 way 1 shot (left) and 5 shot (right) setting on miniImagenet.

529 We note that the mean attention score is always 0.25 as we follow a meta-batch size of 4. We observe
 530 that the TA module’s output follows an interesting trend. Initially, the TA module assigns almost uniform
 531 weights to all the tasks of a batch; however, as the iterations increase, it assigns unequal scores to the tasks
 532 in a batch, preferring some over the other. This suggests that during the initial phases of the meta-model’s
 533 training, all tasks have equal contribution towards learning a *generic structure* of the meta-knowledge.
 534 As the meta-model’s learning proceeds, learning the further *fine-grained meta-knowledge structure* requires
 535 prioritizing some tasks in a batch over the others, which are potentially better aligned with learning the
 536 optimal meta-knowledge. **We study the computational burden imposed by TA regimen in the appendix.**

537 We further decipher the functioning of
 538 the black box attention network by an-
 539 alyzing the qualitative relation among
 540 weights and the classes of task batches
 541 (Figure 6). In Figure 6 left column (col-
 542 1) corresponds to the cases where the as-
 543 signment of attention scores to the tasks
 544 is human interpretable. In contrast, the
 545 right column (col-2) refers to the uninter-
 546 pretable attention scores. From the hu-
 547 man perspective, tasks containing images
 548 from similar classes are hard to distin-
 549 guish and are assigned higher attention
 550 scores indicated by red bounding boxes
 551 (Figure 6 col-1). Specifically, (col-1, row-
 552 1) task 2 is regarded as most important,
 553 possibly because it includes three breeds of dogs followed by task 4, which comprises two species of fish.
 554 However, the aforementioned is not a hard constraint, as there are some task batches (Figure 6 col-2) in
 555 which the distribution of weights cannot be explained qualitatively.



556 Figure 5: Trend of an attention vector in 5 way 1 shot (left) and
 557 5 shot (right) settings on miniImagenet dataset for TA-MAML*.
 558

559

560

561

562

563

564

565

566

567

568

569

570

571

572

573

574

575

576

577

6 Conclusion

In this work we have shown that the batch wise episodic training regimen adopted by ML strategies can benefit from leveraging knowledge about the importance of tasks within a batch. Unlike prior approaches that assume uniform importance for each task in a batch, we propose task attention as a way to learn the relevance of each task according to its alignment with the optimal meta-knowledge. We have validated the effectiveness of task attention by augmenting it to popular initialization and optimization based ML strategies. We have demonstrated through experiments on miniImagenet, FC100 and tieredImageNet datasets that augmenting task attention helps attain better generalization to unseen tasks from the same distribution while requiring fewer iterations to converge. We also show that the task attention is meritorious over existing task scheduling algorithms, even on noisy and CDFSL setups. We also conduct an exhaustive empirical analysis on the distribution of attention weights to study the nature of the meta-knowledge and task attention module. We leave the theoretical motivation of the meta-information components and the proof of convergence of the proposed curriculum as part of our future work. We believe that this end-to-end attention-based meta training paves the way towards efficient and automated meta-training.

7 Broader Impact

We acknowledge that transfer and metric approaches like (Kolesnikov et al., 2020; Triantafillou et al., 2019; Bronskill et al., 2021; Dvornik et al., 2020) use more advanced backbones and our approach is limited to a basic architecture (Conv4) and gradient-based methods. We clarify that though our approach is extendable to any episodic curriculum (including metric approaches with minor design changes), we choose gradient-based approaches like MAML and ANIL approaches as they are domain-agnostic in contrast to metric learning. However, we leave the investigation of attention mechanisms for metric approaches and domains, such as reinforcement learning or regression problems for gradient approaches for future work. Unfortunately, due

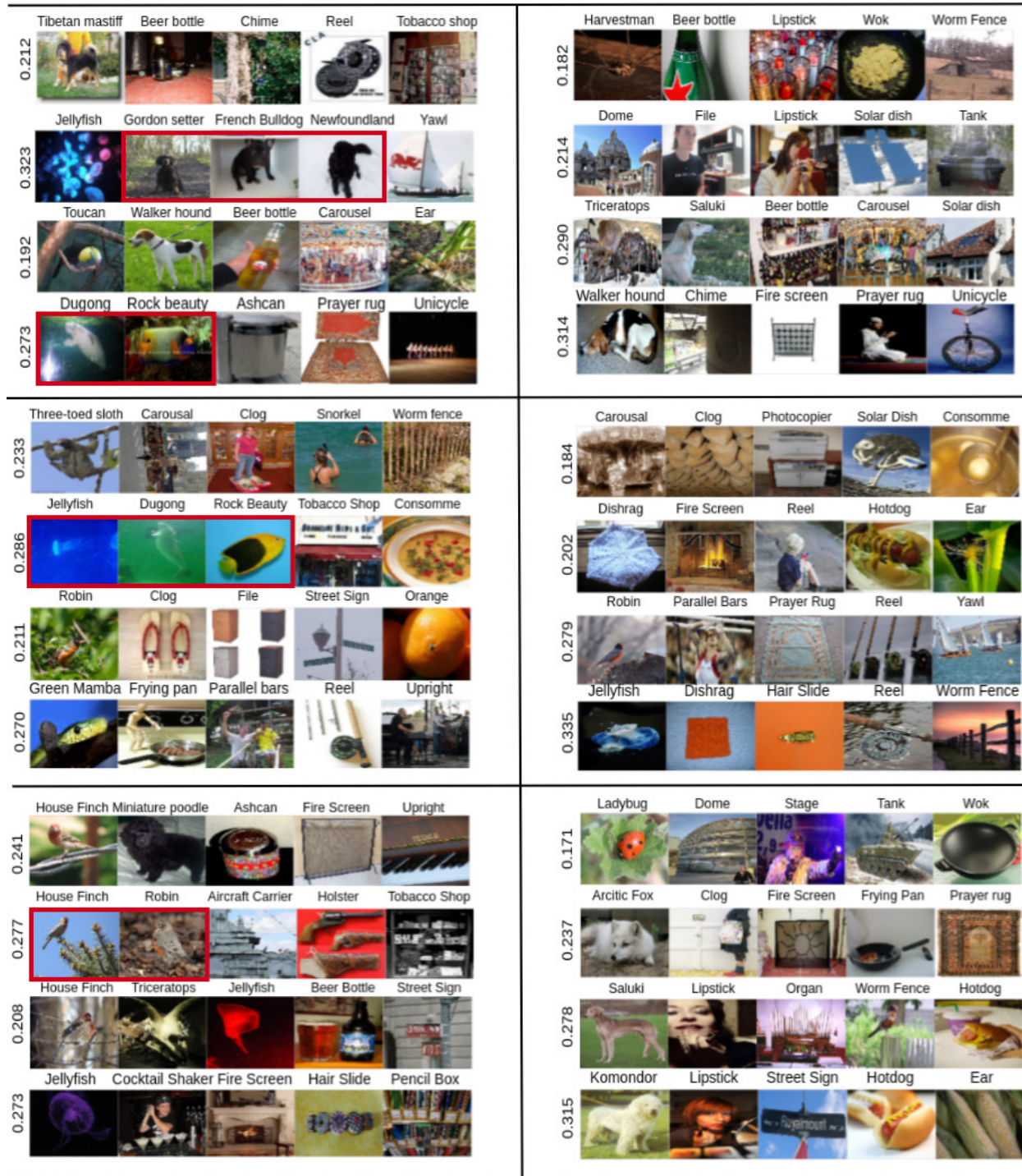


Figure 6: Explanations of TA module in TA-MAML* on miniImagenet. **Left Col)** Higher weights accredited to tasks with comparable classes marked by red bounding boxes. **Right Col)** Association of weights and task data is qualitatively uninterpretable. Rows correspond to the batches.

578 to computational and storage restrictions, we are unable to experiment with deeper backbones and large
579 image sizes for gradient-based methods. We, therefore, limit the scope of our study only to algorithms,

580 datasets, and conditions and leave the scalability aspect to the future. We, however, point out the existing
 581 literature (Chen et al., 2018) that compares vanilla transfer learning (with no Imagenet pretraining or data
 582 augmentation) for conv4 backbone with episodic training (MAML) under fair conditions. Chen et al. have
 583 demonstrated that MAML performs better than vanilla transfer learning under fair conditions for conv4
 584 architecture. However, transfer learning scales much better with the architectures than MAML (or other
 585 episodic methods) (Chen et al., 2018). Nevertheless, transfer learning (TL) is a good solution for few-shot
 586 learning (especially with Imagenet pretraining and larger backbones), and translating attention to TL for
 587 a few-shot setup is a promising direction for further research. An attention module, in this case, could be
 588 used to reweigh the examples instead of tasks, and it could be trained using a smaller validation data pool.
 589 Also, sampling a validation pool from a combination of distributions (transduction) is worth exploring. We
 590 leave these extensions for future work. We, acknowledge, that similar to (Yao et al., 2021; Wu et al., 2022;
 591 Raghu et al., 2020), our study is limited to understanding the fundamentals of episodic training rather than
 592 developing an algorithm that surpasses the state-of-the-art approach for few shot learning.

593 References

- 594 Mayank Agarwal, Mikhail Yurochkin, and Yuekai Sun. On sensitivity of meta-learning to support data.
 595 *Advances in Neural Information Processing Systems*, 34:20447–20460, 2021.
- 596 Aroof Aimen, Sahil Sidhekh, Vineet Madan, and Narayanan C Krishnan. Stress Testing of Meta-learning
 597 Approaches for Few-shot Learning. In *AAAI Workshop on Meta-Learning and MetaDL Challenge*, 2021.
- 598 Antreas Antoniou, Harri Edwards, and Amos Storkey. How to train your maml. In *Seventh International
 599 Conference on Learning Representations*, 2019.
- 600 Sébastien Arnold, Guneet Dhillon, Avinash Ravichandran, and Stefano Soatto. Uniform sampling over
 601 episode difficulty. *Advances in Neural Information Processing Systems*, 34:1481–1493, 2021.
- 602 Sébastien MR Arnold, Praateek Mahajan, Debajyoti Datta, Ian Bunner, and Konstantinos Saitas Zarkias.
 603 learn2learn: A library for meta-learning research. *CoRR*, 2020.
- 604 Yoshua Bengio, Jérôme Louradour, Ronan Collobert, and Jason Weston. Curriculum learning. In *Proceed-
 605 ings of the 26th Annual International Conference on Machine Learning, ICML 2009, Montreal, Quebec,
 606 Canada, June 14-18, 2009*, volume 382 of *ACM International Conference Proceeding Series*, pp. 41–48.
 607 ACM, 2009.
- 608 John Bronskill, Daniela Massiceti, Massimiliano Patacchiola, Katja Hofmann, Sebastian Nowozin, and
 609 Richard Turner. Memory efficient meta-learning with large images. *Advances in Neural Information
 610 Processing Systems*, 34:24327–24339, 2021.
- 611 Haw-Shiuan Chang, Erik G. Learned-Miller, and Andrew McCallum. Active bias: Training more accurate
 612 neural networks by emphasizing high variance samples. In *Advances in Neural Information Processing
 613 Systems 30: Annual Conference on Neural Information Processing Systems 2017, December 4-9, 2017,
 614 Long Beach, CA, USA*, pp. 1002–1012, 2017.
- 615 Wei-Yu Chen, Yen-Cheng Liu, Zsolt Kira, Yu-Chiang Frank Wang, and Jia-Bin Huang. A closer look at
 616 few-shot classification. In *International Conference on Learning Representations*, 2018.
- 617 Guneet Singh Dhillon, Pratik Chaudhari, Avinash Ravichandran, and Stefano Soatto. A baseline for few-shot
 618 image classification. In *International Conference on Learning Representations*, 2019.
- 619 Vincent Dumoulin, Neil Houlsby, Utku Evci, Xiaohua Zhai, Ross Goroshin, Sylvain Gelly, and Hugo
 620 Larochelle. A unified few-shot classification benchmark to compare transfer and meta learning approaches.
 621 In *Thirty-fifth Conference on Neural Information Processing Systems Datasets and Benchmarks Track
 622 (Round 1)*, 2021.
- 623 Nikita Dvornik, Cordelia Schmid, and Julien Mairal. Selecting relevant features from a multi-domain repre-
 624 sentation for few-shot classification. In *European Conference on Computer Vision*, pp. 769–786. Springer,
 625 2020.

- 626 Chelsea Finn, Pieter Abbeel, and Sergey Levine. Model-agnostic meta-learning for fast adaptation of deep
627 networks. In *ICML*, 2017.
- 628 Yunhui Guo, Noel C Codella, Leonid Karlinsky, James V Codella, John R Smith, Kate Saenko, Tajana
629 Rosing, and Rogerio Feris. A broader study of cross-domain few-shot learning. In *European conference on*
630 *computer vision*, pp. 124–141. Springer, 2020.
- 631 Ricardo Luna Gutierrez and Matteo Leonetti. Information-theoretic task selection for meta-reinforcement
632 learning. In *Advances in Neural Information Processing Systems 33: Annual Conference on Neural Infor-*
633 *mation Processing Systems 2020, NeurIPS 2020, December 6-12, 2020, virtual*, 2020.
- 634 Sepp Hochreiter and Jürgen Schmidhuber. Long short-term memory. *Neural computation*, 1997.
- 635 Muhammad Abdullah Jamal and Guo-Jun Qi. Task agnostic meta-learning for few-shot learning. In *IEEE*
636 *Conference on Computer Vision and Pattern Recognition, CVPR 2019, Long Beach, CA, USA, June*
637 *16-20, 2019*, pp. 11719–11727. Computer Vision Foundation / IEEE, 2019.
- 638 Lu Jiang, Zhengyuan Zhou, Thomas Leung, Li-Jia Li, and Li Fei-Fei. Mentornet: Learning data-driven
639 curriculum for very deep neural networks on corrupted labels. In *Proceedings of the 35th International*
640 *Conference on Machine Learning, ICML 2018, Stockholmsmässan, Stockholm, Sweden, July 10-15, 2018*,
641 volume 80 of *Proceedings of Machine Learning Research*, pp. 2309–2318. PMLR, 2018.
- 642 Jean Kaddour, Steindór Sæmundsson, and Marc Peter Deisenroth. Probabilistic active meta-learning. In
643 *Advances in Neural Information Processing Systems 33: Annual Conference on Neural Information Pro-*
644 *cessing Systems 2020, NeurIPS 2020, December 6-12, 2020, virtual*, 2020.
- 645 H. Kahn and A. W. Marshall. Methods of reducing sample size in monte carlo computations. *Oper. Res.*,
646 1953.
- 647 Diederik P. Kingma and Jimmy Ba. Adam: A method for stochastic optimization. In *3rd International*
648 *Conference on Learning Representations, ICLR 2015, San Diego, CA, USA, May 7-9, 2015, Conference*
649 *Track Proceedings*, 2015.
- 650 Alexander Kolesnikov, Lucas Beyer, Xiaohua Zhai, Joan Puigcerver, Jessica Yung, Sylvain Gelly, and Neil
651 Houlsby. Big transfer (bit): General visual representation learning. In *European conference on computer*
652 *vision*, pp. 491–507. Springer, 2020.
- 653 M. Pawan Kumar, Benjamin Packer, and Daphne Koller. Self-paced learning for latent variable models. In
654 *Advances in Neural Information Processing Systems 23: 24th Annual Conference on Neural Information*
655 *Processing Systems 2010. Proceedings of a meeting held 6-9 December 2010, Vancouver, British Columbia,*
656 *Canada*, pp. 1189–1197. Curran Associates, Inc., 2010.
- 657 Jian Li, Xuanyuan Luo, and Mingda Qiao. On generalization error bounds of noisy gradient methods for
658 non-convex learning. In *International Conference on Learning Representations*, 2019.
- 659 Zhenguo Li, Fengwei Zhou, Fei Chen, and Hang Li. Meta-sgd: Learning to learn quickly for few-shot learning,
660 2017.
- 661 Tsung-Yi Lin, Priya Goyal, Ross B. Girshick, Kaiming He, and Piotr Dollár. Focal loss for dense object
662 detection. In *IEEE International Conference on Computer Vision, ICCV 2017, Venice, Italy, October*
663 *22-29, 2017*, pp. 2999–3007. IEEE Computer Society, 2017.
- 664 Bo Liu, Xingchao Liu, Xiaojie Jin, Peter Stone, and Qiang Liu. Conflict-averse gradient descent for multi-task
665 learning. *Advances in Neural Information Processing Systems*, 34:18878–18890, 2021a.
- 666 Chenghao Liu, Zhihao Wang, Doyen Sahoo, Yuan Fang, Kun Zhang, and Steven C. H. Hoi. Adaptive task
667 sampling for meta-learning. In *ECCV*, 2020.

- 668 Evan Z Liu, Behzad Haghgoo, Annie S Chen, Aditi Raghunathan, Pang Wei Koh, Shiori Sagawa, Percy Liang,
 669 and Chelsea Finn. Just train twice: Improving group robustness without training group information. In
 670 *ICML*, 2021b.
- 671 Jaehoon Oh, Hyungjun Yoo, ChangHwan Kim, and Se-Young Yun. Boil: Towards representation change for
 672 few-shot learning. In *International Conference on Learning Representations*, 2020.
- 673 Boris N. Oreshkin, Pau Rodríguez López, and Alexandre Lacoste. TADAM: task dependent adaptive metric
 674 for improved few-shot learning. In *Advances in Neural Information Processing Systems 31: Annual Con-
 675 ference on Neural Information Processing Systems 2018, NeurIPS 2018, December 3-8, 2018, Montréal,
 676 Canada*, pp. 719–729, 2018.
- 677 Aniruddh Raghu, Maithra Raghu, Samy Bengio, and Oriol Vinyals. Rapid learning or feature reuse? towards
 678 understanding the effectiveness of MAML. In *8th International Conference on Learning Representations,
 679 ICLR 2020, Addis Ababa, Ethiopia, April 26-30, 2020*. OpenReview.net, 2020.
- 680 Sachin Ravi and Hugo Larochelle. Optimization as a model for few-shot learning. In *5th International
 681 Conference on Learning Representations, ICLR 2017, Toulon, France, April 24-26, 2017, Conference
 682 Track Proceedings*. OpenReview.net, 2017.
- 683 Mengye Ren, Eleni Triantafillou, Sachin Ravi, Jake Snell, Kevin Swersky, Joshua B. Tenenbaum, Hugo
 684 Larochelle, and Richard S. Zemel. Meta-learning for semi-supervised few-shot classification. In *6th Inter-
 685 national Conference on Learning Representations, ICLR 2018, Vancouver, BC, Canada, April 30 - May
 686 3, 2018, Conference Track Proceedings*. OpenReview.net, 2018a.
- 687 Mengye Ren, Wenyuan Zeng, Bin Yang, and Raquel Urtasun. Learning to reweight examples for robust
 688 deep learning. In *Proceedings of the 35th International Conference on Machine Learning, ICML 2018,
 689 Stockholmsmässan, Stockholm, Sweden, July 10-15, 2018*, volume 80 of *Proceedings of Machine Learning
 690 Research*, pp. 4331–4340. PMLR, 2018b.
- 691 Andrei A. Rusu, Dushyant Rao, Jakub Sygnowski, Oriol Vinyals, Razvan Pascanu, Simon Osindero, and
 692 Raia Hadsell. Meta-learning with latent embedding optimization. In *7th International Conference on
 693 Learning Representations, ICLR 2019, New Orleans, LA, USA, May 6-9, 2019*. OpenReview.net, 2019.
- 694 Jaewoong Shin, Hae Beom Lee, Boqing Gong, and Sung Ju Hwang. Large-scale meta-learning with continual
 695 trajectory shifting. In *International Conference on Machine Learning*, pp. 9603–9613. PMLR, 2021.
- 696 Abhinav Shrivastava, Abhinav Gupta, and Ross B. Girshick. Training region-based object detectors with
 697 online hard example mining. In *2016 IEEE Conference on Computer Vision and Pattern Recognition,
 698 CVPR 2016, Las Vegas, NV, USA, June 27-30, 2016*, pp. 761–769. IEEE Computer Society, 2016.
- 699 Qianru Sun, Yaoyao Liu, Tat-Seng Chua, and Bernt Schiele. Meta-transfer learning for few-shot learning.
 700 In *IEEE Conference on Computer Vision and Pattern Recognition, CVPR 2019, Long Beach, CA, USA,
 701 June 16-20, 2019*, pp. 403–412. Computer Vision Foundation / IEEE, 2019.
- 702 Qianru Sun, Yaoyao Liu, Zhaozheng Chen, Tat-Seng Chua, and Bernt Schiele. Meta-transfer learning through
 703 hard tasks. *IEEE Transactions on Pattern Analysis and Machine Intelligence*, 2020.
- 704 Eleni Triantafillou, Tyler Zhu, Vincent Dumoulin, Pascal Lamblin, Utku Evci, Kelvin Xu, Ross Goroshin,
 705 Carles Gelada, Kevin Swersky, Pierre-Antoine Manzagol, et al. Meta-dataset: A dataset of datasets for
 706 learning to learn from few examples. In *International Conference on Learning Representations*, 2019.
- 707 Oriol Vinyals, Charles Blundell, Tim Lillicrap, Koray Kavukcuoglu, and Daan Wierstra. Matching networks
 708 for one shot learning. In *Advances in Neural Information Processing Systems 29: Annual Confer-
 709 ence on Neural Information Processing Systems 2016, December 5-10, 2016, Barcelona, Spain*, pp. 3630–3638,
 710 2016.
- 711 Yichen Wu, Long-Kai Huang, and Ying Wei. Adversarial task up-sampling for meta-learning. In *Advances
 712 in Neural Information Processing Systems*, 2022.

- 713 Huaxiu Yao, Yu Wang, Ying Wei, Peilin Zhao, Mehrdad Mahdavi, Defu Lian, and Chelsea Finn. Meta-
714 learning with an adaptive task scheduler. *Advances in Neural Information Processing Systems*, 2021.
- 715 Xiaohua Zhai, Joan Puigcerver, Alexander Kolesnikov, Pierre Ruyssen, Carlos Riquelme, Mario Lucic, Josip
716 Djolonga, Andre Susano Pinto, Maxim Neumann, Alexey Dosovitskiy, et al. A large-scale study of repre-
717 sentation learning with the visual task adaptation benchmark. *arXiv preprint arXiv:1910.04867*, 2019.
- 718 Peilin Zhao and Tong Zhang. Stochastic optimization with importance sampling for regularized loss mini-
719 mization. In *Proceedings of the 32nd International Conference on Machine Learning, ICML 2015, Lille,*
720 *France, 6-11 July 2015*, volume 37 of *JMLR Workshop and Conference Proceedings*, pp. 1–9. JMLR.org,
721 2015.

722 8 Appendix

723 8.1 Preliminary

724 8.1.1 Meta-knowledge as an Optimal Initialization

725 When meta-knowledge is a generic initialization on the model parameters learned through the experience
 726 over various tasks, it is enforced to be close to each individual training tasks' optimal parameters. A model
 727 initialized with such an optimal prior quickly adapts to unseen tasks from the same distribution during
 728 meta-testing. **MAML** (Finn et al., 2017) employs a nested iterative process to learn the task-agnostic
 729 optimal prior θ . In the inner iterations representing the task adaptation steps, θ is separately fine-tuned for
 730 each meta-training task \mathcal{T}_i of a batch using D_i to obtain ϕ_i through gradient descent on the train loss L
 731 using learning rate α . Specifically, ϕ_i is initialized as θ and updated using $\phi_i \leftarrow \phi_i - \alpha \nabla_{\phi_i} L(\phi_i)$, T times
 732 resulting in the adapted model ϕ_i^T . In the outer loop, meta-knowledge is gathered by optimizing θ over
 733 loss L^* computed with the task adapted model parameters ϕ_i^T on query dataset D_i^* . Specifically, during
 734 meta-optimization $\theta \leftarrow \theta - \beta \nabla_\theta \sum_{i=1}^B L^*(\phi_i^T)$ using a task batch of size B and learning rate β . **MetaSGD**
 735 (Li et al., 2017) improves upon MAML by learning parameter-specific learning rates α in addition to the
 736 optimal initialization in a similar nested iterative procedure. Meta-knowledge is gathered by optimizing θ
 737 and α in the outer loop using the loss L^* computed on query set D_i^* . Specifically, during meta-optimization
 738 $(\theta, \alpha) \leftarrow (\theta, \alpha) - \beta \nabla_{(\theta, \alpha)} \sum_{i=1}^B L^*(\phi_i^T)$. Learning dynamic learning rates for each parameter of a model
 739 makes MetaSGD faster and more generalizable than MAML. A single adaptation step is sufficient to adjust
 740 the model towards a new task. The performance of MAML is attributed to the reuse of the features
 741 across tasks rather than the rapid learning of new tasks (Raghu et al., 2020). Exploiting this characteristic,
 742 **ANIL** freezes the feature backbone layers ($1, \dots, l-1$) and only adapts classifier layer (l) in the inner
 743 loop T times. Specifically during adaptation $\phi_i^l \leftarrow \phi_i^l - \alpha \nabla_{\phi_i^l} L(\phi_i^l)$. During meta-optimization $\theta^{1, \dots, l} \leftarrow$
 744 $\theta^{1, \dots, l} - \beta \nabla_{\theta^{1, \dots, l}} \sum_{i=1}^B L^*(\phi_i^{lT})$ i.e., all layers are learned in the outer loop. Freezing the feature backbone
 745 during adaptation reduces the overhead of computing gradient through the gradient (differentiating through
 746 the inner loop), and thereby heavier backbones could be used for the feature extraction. **TAML** (Jamal
 747 & Qi, 2019) suggests that the optimal prior learned by MAML may still be biased towards some tasks.
 748 They propose to reduce this bias and enforce equity among the tasks by explicitly minimizing the inequality
 749 among the performances of tasks in a batch. The inequality defined using statistical measures such as Theil
 750 Index, Atkinson Index, Generalized Entropy Index, and Gini Coefficient among the performances of tasks
 751 in a batch is used as a regularizer while gathering the meta-knowledge. For the baseline comparison, in
 752 our experiments, we use the Theil index for TAML owing to its average best results. Specifically during
 753 meta-optimization $\theta \leftarrow \theta - \beta \nabla_\theta \left[\sum_{i=1}^B L^*(\phi_i^T) + \lambda \left\{ \frac{L^*(\phi_i^0)}{\bar{L}^*(\phi_i^0)} \ln \frac{L^*(\phi_i^0)}{\bar{L}^*(\phi_i^0)} \right\} \right]$ (for TAML-Theil Index) where B
 754 is the number of tasks in a batch, $L^*(\phi_i^0)$ is the loss incurred by initial model ϕ_i^0 on the query set D_i^* of
 755 task \mathcal{T}_i and $\bar{L}^*(\phi_i^0)$ is the average query loss of initial model on a batch of tasks. As TAML enforces equity
 756 of the optimal prior towards meta-train tasks, it counters the adaptation, which leads to slow and unstable
 757 training largely dependent on λ .

758 8.1.2 Meta-knowledge as a Parametric Optimizer

759 A regulated gradient-based optimizer gathers the task-specific and task-agnostic meta-knowledge to traverse
 760 the loss surfaces of tasks in the meta-train set during meta-training. A base model guided by such a
 761 learned parametric optimizer quickly finds the way to minima even for unseen tasks sampled from the
 762 same distribution during meta-testing. **MetaLSTM** (Ravi & Larochelle, 2017) is a recurrent parametric
 763 optimizer θ that mimics the gradient-based optimization of a base model ϕ . This recurrent optimizer is an
 764 LSTM (Hochreiter & Schmidhuber, 1997) and is inherently capable of performing two-level learning due to its
 765 architecture. During adaptation of ϕ_i on D_i , θ takes meta information of ϕ_i characterized by its current loss
 766 L and gradients $\nabla_{\phi_i}(L)$ as input and outputs the next set of parameters for ϕ_i . This adaptation procedure
 767 is repeated T times resulting in the adapted base-model ϕ_i^T . Internally, the cell state of θ corresponds to ϕ_i ,
 768 and the cell state update for θ resembles a learned and controlled gradient update. The emphasis on previous
 769 parameters and the current update is regulated by the learned forget and input gates respectively. While

adapting ϕ_i to D_i , information about the trajectory on the loss surface across the adaptation steps is captured in the hidden states of θ , representing the task-specific knowledge. During meta-optimization, θ is updated based on the loss of the adapted model $L^*(\phi_i^T)$ computed on the query set D_i^* to garner the meta-knowledge across tasks. Specifically, during meta-optimization, $\theta \leftarrow \theta - \beta \nabla_\theta L^*(\phi_i^T)$. MetaLSTM updates parametric optimizer θ after adapting the base model ϕ to each task. This causes θ to follow optima's of all adapted base models leading to its elongated and fluctuating optimization trajectory, which is biased towards the last task. **MetaLSTM++** (Aimen et al., 2021) circumvents these issues as θ is updated by an aggregate query loss of the adapted models on a batch of tasks. Batch updates smoothen the optimization trajectory of θ and eliminate its bias towards the last task. Specifically, during meta-optimization $\theta \leftarrow \theta - \beta \nabla_\theta \sum_{i=1}^B L^*(\phi_i^T)$.

8.2 Detailed Explanation of the Proposed approach

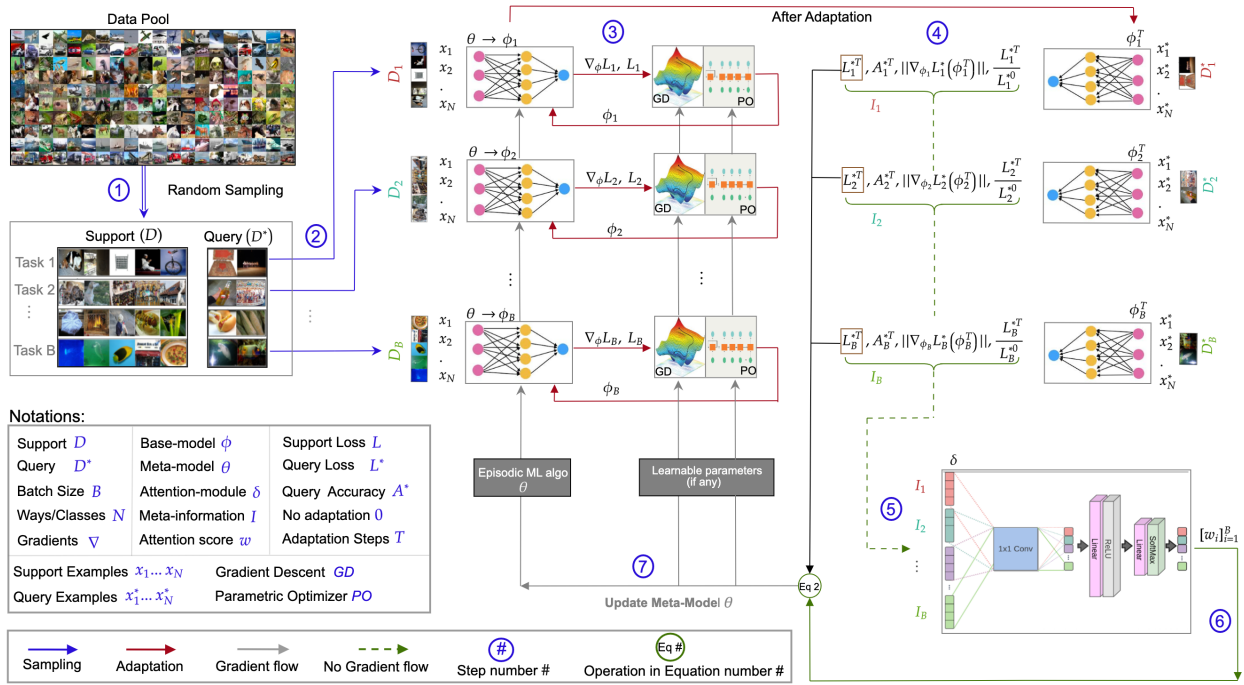


Figure 7: [Best viewed in color] Workflow of proposed training curriculum.

We explain the proposed approach through Figure 1, Figure 7, Algorithm 1, and equations. We first sample a batch of tasks (B) from a random pool of data (Figure 7 - Label ①). For each task, the base-model ϕ_i is adapted using the support data D_i for T time-steps (line 7 and lines 20-32 in Algorithm 1, Figure 7 - Label ③). Specifically, the adaptation is done using gradient descent on the train loss L for initialization approaches (lines 22-26 in Algorithm 1, Figure 7 - GD), or the current loss and gradients are inputted to the meta-model θ for optimization approaches, which then outputs the updated base-model parameters (lines 27-31 in Algorithm 1, Figure 7 - PO). The meta-information (I) corresponding to each task in the batch is then calculated (Figure 7 - Label ④), which includes the loss, accuracy, loss-ratio, and gradient norm of adapted models on the query data. This is given as input to the task attention module (Figure 1 - Label ②, Figure 7 - Label ⑤), which outputs the attention vector (line 10 in Algorithm 1, Figure 7 - Label ⑥). The attention vector and test losses are used to update the meta-model parameters θ according to equation 2 (line 11 in Algorithm 1, Figure 1 - Label ④, Figure 7 - Label ⑦). A new batch of tasks is then sampled and the base-models are adapted using the updated meta-model (Lines 12-16 in Algorithm 1, Figure 1 - Label ⑤). The mean test loss over the adapted base-models is calculated and used to update the parameters of the task attention module δ according to equation 3.

795 **8.3 Experiments**796 **8.3.1 Datasets Details**

797 **miniImagenet** dataset (Vinyals et al., 2016) comprises 600 color images of size 84×84 from each of
 798 100 classes sampled from the Imagenet dataset. The 100 classes are split into 64, 16 and 20 classes for
 799 meta-training, meta-validation and meta-testing respectively. **miniImagenet-noisy** (Yao et al., 2021) is
 800 constructed from the miniImagenet dataset with the additional constraint that tasks have noisy support
 801 labels and clean query labels. The noise in support labels is introduced by symmetry flipping, and the default
 802 noise ratio is 0.6. **Fewshot Cifar 100 (FC100)** dataset (Oreshkin et al., 2018) has been created from Cifar
 803 100 object classification dataset. It contains 600 color images of size 32×32 corresponding to each of 100
 804 classes grouped into 20 super-classes. Among 100 classes, 60 classes belonging to 12 super-classes correspond
 805 to the meta-train set, 20 classes from 4 super-classes to the meta-validation set, and the rest to the meta-test
 806 set. **tieredImageNet** (Ren et al., 2018a) is a more challenging benchmark for few-shot image classification.
 807 It contains 779,165 color images sampled from 608 classes of Imagenet and are grouped into 34 super-
 808 classes. These super-classes are divided into 20, 6, and 8 disjoint sets for meta-training, meta-validation,
 809 and meta-testing. **Metadataset** (Triantafillou et al., 2019) comprises of 10 freely available diverse datasets
 810 - Aircraft, CUB-200-2011, Describable Textures, Fungi, ILSVRC-2012, MSCOCO, Omniglot, Quick Draw,
 811 Traffic Signs, and VGG Flower. We utilized CUB-200, FGVC-Aircraft, Describable Textures, and Omniglot
 812 datasets from Metadataset. **VTAB dataset** (Zhai et al., 2019) is a more diverse dataset than Metadataset
 813 that was proposed to avoid overlapping classes of sub-datasets with the Imagenet dataset. VTAB comprises
 814 of 19 datasets divided into three domains - Natural, Specialized, and Structured, depending on the type of
 815 images. The natural group contains Caltech101, CIFAR100, DTD, Flowers102, Pets, Sun397, and SVHN
 816 sub-datasets, while the specialized group consists of remote sensing datasets like EuroSAT and Resisc45
 817 and medical datasets like Retinopathy and Patch Camelyon. Structured contains object counting or 3D
 818 depth prediction datasets like Clevr/count, Clevr/distance, dSprites/location, dSprites/orientation, Small-
 819 NORB/azimuth, SmallNORB/elevation, DMLab, and KITTI/distance. We considered Natural sub-datasets
 820 like DTD, CIFAR FC 100, Flowers102, and SVHN, specialized sub-datasets like EuroSAT and Resisc45, and
 821 structured sub-datasets like dSprites_location and dSprites_orientation for cross-domain experimentation.
 822 According to (Dumoulin et al., 2021), we have kept Describable Textures as a part of Metadataset and
 823 Flowers102 as a component of the VTAB dataset.

824 **8.3.2 Ablation Studies**

825 We analyze the ranks of the tasks for maximum and minimum values of : loss, loss ratio, accuracy, and grad
 826 norm in a batch wrt attention weights throughout meta-training of TA-MAML on a 5 way 1 and 5 shot
 827 settings on miniImagenet dataset (Figures 8 and 9). Specifically, the highest weighted task is given rank
 828 one, and the least weighted task in a batch is given the last rank. We observe that the TA module does not
 829 assign maximum weight to the tasks with maximum or minimum values of : test loss, loss ratio, grad norm
 830 or accuracy throughout meta-training. Thus, the TA module does not trivially learn to assign weights to
 831 the tasks based on some component of meta-information but learns useful latent information from all the
 832 components to assign importance for the tasks in a batch.

833 **8.3.3 Relation of Weights with Meta-Information**

834 In Figure 10, we illustrate the trend of mean weighted loss across iterations for TA-MAML on 5 way 1 and
 835 5 shot settings on miniImagenet dataset. The trend indicates that the average weighted loss decreases over
 836 the meta-training iterations. The shaded region represents a 95% confidence interval over 100 tasks.

837 **8.3.4 Computational Overhead**

838 The training time for all scheduling/sampling approaches is expected to be higher than their non-
 839 scheduling/sampling counterparts. We observe a three-fold increase in the training time from the vanilla
 840 setting for a model trained with our strategy and a two-fold increase in the training time if a non-neural
 841 scheduling approach (Liu et al., 2021a) is employed. However, our approach significantly outperforms vanilla

5 way 1 shot setting

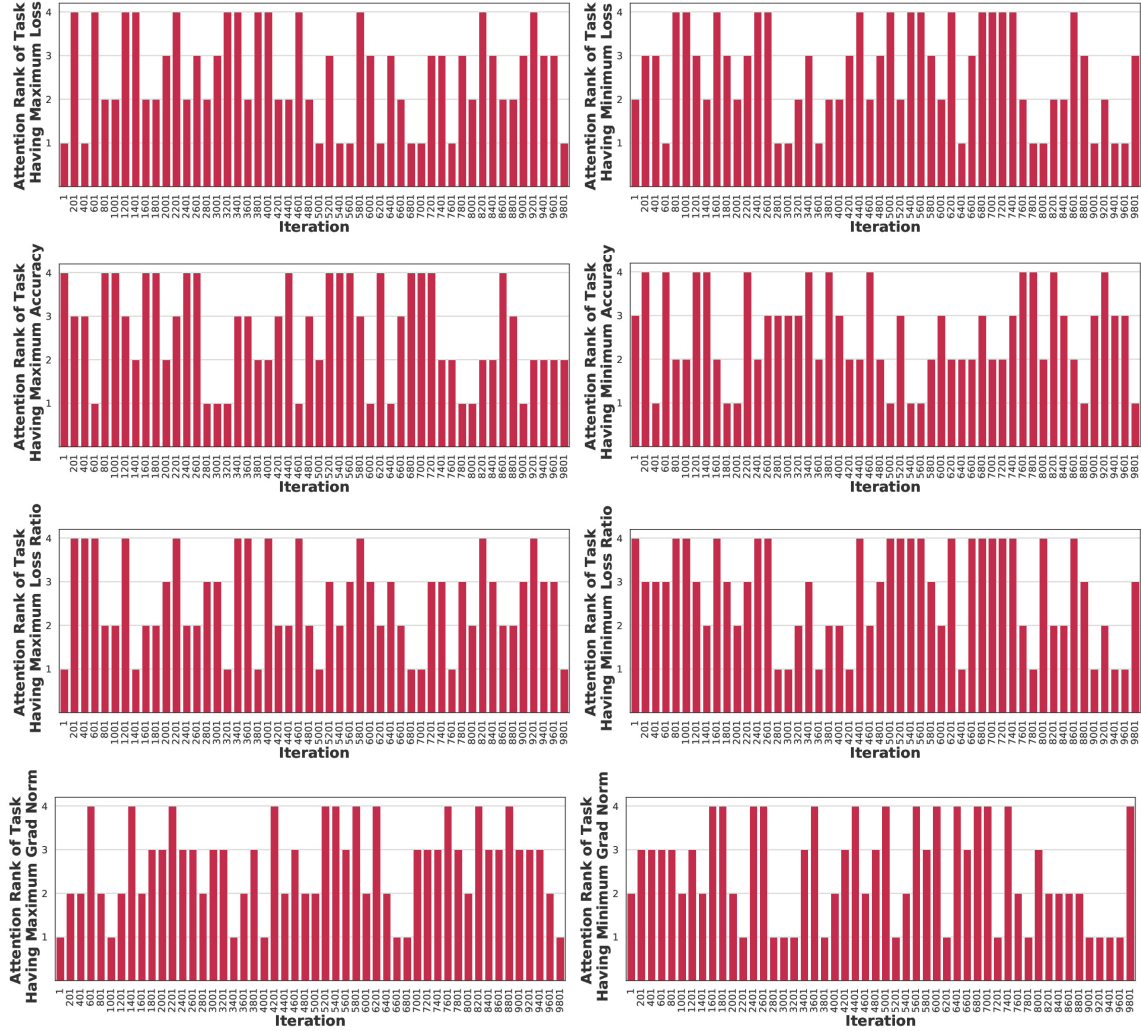


Figure 8: Rank Analysis of tasks for maximum and minimum values of : loss, loss-ratio, accuracy and grad norm throughout the training of TA-MAML* for 5 way 1 shot setting on miniImagenet dataset.

Table 7: Comparison of few-shot classification performance of MAML and ANIL reported in the original papers (denoted by #) and the re-implementation by others on miniImagenet dataset for 5 way 1 and 5 shot settings. The highest and lowest accuracies for an approach are represented in blue and red, respectively.

| Model | Test Accuracy (%) | |
|------------------------------|-------------------|--------------------|
| | 5 Way | |
| | 1 Shot | 5 Shot |
| miniImagenet | | |
| MAML#(Finn et al., 2017) | 48.07 \pm 1.75 | 63.15 \pm 0.91 - |
| MAML (Antoniou et al., 2019) | 48.25 \pm 0.62 | 64.39 \pm 0.31 |
| MAML (Raghu et al., 2020) | 46.9 \pm 0.2 | 63.1 \pm 0.4- |
| MAML (Chen et al., 2018) | 46.47 \pm 0.82 | 62.71 \pm 0.71 |
| MAML(Oh et al., 2020) | 47.44 \pm 0.23 | 61.75 \pm 0.42 |
| MAML (Agarwal et al., 2021) | 47.13 \pm 8.78 | 57.69 \pm 7.92 |
| MAML (Arnold et al., 2021) | 46.88 \pm 0.60 | 55.16 \pm 0.55 |
| ANIL#(Raghu et al., 2020) | 46.7 \pm 0.4 | 61.5 \pm 0.5 |
| ANIL(Oh et al., 2020) | 47.82 \pm 0.20 | 63.04 \pm 0.42 |
| ANIL(Arnold et al., 2021) | 46.59 \pm 0.60 | 63.47 \pm 0.55 |

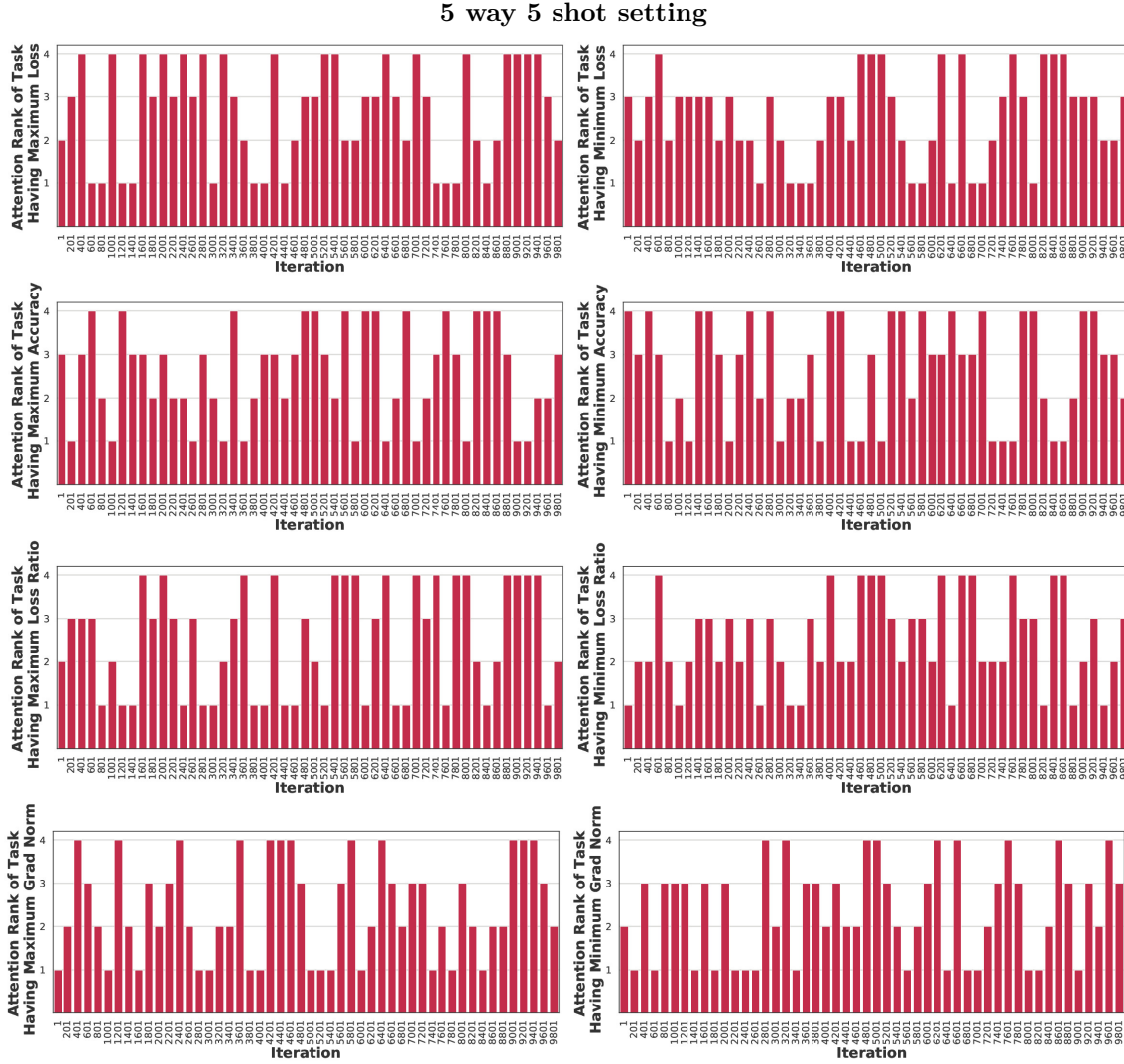


Figure 9: Rank Analysis of tasks for maximum and minimum values of : loss, loss-ratio, accuracy and grad norm throughout the training of TA-MAML* for 5 way 5 shot setting on miniImagenet dataset.

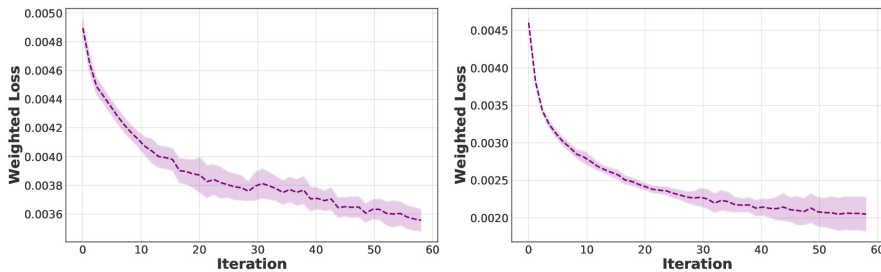


Figure 10: Trend analysis of weighted loss across meta-training iterations for TA-MAML* on 5 way 1 shot (left) and 5 shot (right) settings on miniImagenet dataset. Iterations are in thousands.

842 ML approaches and all state-of-the-art scheduling strategies on various datasets, training setups, and learn-
843 ing paradigms (Tables 2, 3, 4 and 5). As training is typically performed offline, the increased computational
844 overhead is expected to be permissible. Further, ours, as well as other approaches, perform vanilla finetuning
845 during meta-testing (i.e., task attention, neural scheduling or conflict resolving mechanism is not employed
846 during meta-testing), resulting in comparable test time (15-20 seconds on 300 tasks for MAML 5-way 1-
847 and 5-shot setups). We also note that we do not pre-train the attention network, unlike state-of-the-art
848 schedulers like ATS.

⁸⁴⁹ **8.3.5 Hyperparameter Details**

| Setting | Model | base lr | meta lr | attention lr | lambda |
|---------------------|----------------|---------|---------|--------------|--------|
| miniImagenet | | | | | |
| 5.1 | MAML | 0.5000 | 0.0030 | - | - |
| | TAML | 0.5000 | 0.0030 | - | 0.0748 |
| | TA-MAML* | 0.0763 | 0.0005 | 0.0004 | - |
| | MetaSGD | 0.5000 | 0.0030 | - | - |
| | TA-MetaSGD* | 0.0529 | 0.0011 | 0.0004 | - |
| | MetaLSTM | - | 0.005 | - | - |
| | MetaLSTM++ | - | 0.0012 | - | - |
| | TA-MetaLSTM++* | - | 0.0012 | 0.0031 | - |
| | ANIL | 0.3000 | 0.0006 | - | - |
| | TA-ANIL* | 0.0763 | 0.0005 | 0.0004 | - |
| 5.5 | MAML | 0.5000 | 0.0030 | - | - |
| | TAML | 0.5000 | 0.0030 | - | 0.7916 |
| | TA-MAML* | 0.0763 | 0.0005 | 0.0004 | - |
| | MetaSGD | 0.5000 | 0.0030 | - | - |
| | TA-MetaSGD* | 0.0529 | 0.0011 | 0.0004 | - |
| | MetaLSTM | - | 0.005 | - | - |
| | MetaLSTM++ | - | 0.0012 | - | - |
| | TA-MetaLSTM++* | - | 0.0004 | 0.0001 | - |
| | ANIL | 0.3000 | 0.0006 | - | - |
| | TA-ANIL* | 0.0763 | 0.0005 | 0.0004 | - |
| 10.1 | MAML | 0.5000 | 0.0030 | - | - |
| | TAML | 0.5000 | 0.0030 | - | 0.2631 |
| | TA-MAML* | 0.2551 | 0.0015 | 0.0001 | - |
| | MetaSGD | 0.5000 | 0.0030 | - | - |
| | TA-MetaSGD* | 0.0627 | 0.0008 | 0.0013 | - |
| | MetaLSTM | - | 0.005 | - | - |
| | MetaLSTM++ | - | 0.0015 | - | - |
| | TA-MetaLSTM++* | - | 0.0009 | 0.0015 | - |
| | ANIL | 0.5000 | 0.0030 | - | - |
| | TA-ANIL* | 0.2551 | 0.0015 | 0.0001 | - |
| 10.5 | MAML | 0.5000 | 0.0030 | - | - |
| | TAML | 0.5000 | 0.0030 | - | 0.0741 |
| | TA-MAML* | 0.2551 | 0.0015 | 0.0001 | - |
| | MetaSGD | 0.5000 | 0.0030 | - | - |
| | TA-MetaSGD* | 0.0627 | 0.0008 | 0.0013 | - |
| | MetaLSTM | - | 0.005 | - | - |
| | MetaLSTM++ | - | 0.0036 | - | - |
| | TA-MetaLSTM++* | - | 0.0024 | 0.0002 | - |
| | ANIL | 0.5000 | 0.0030 | - | - |
| | TA-ANIL* | 0.2551 | 0.0015 | 0.0001 | - |

| Setting | Model | base lr | meta lr | attention lr | lambda |
|--------------|----------------|---------|---------|--------------|--------|
| FC100 | | | | | |
| 5.1 | MAML | 0.5000 | 0.0030 | - | - |
| | TAML | 0.5000 | 0.0030 | - | 0.0164 |
| | TA-MAML* | 0.2826 | 0.0003 | 0.0024 | - |
| | MetaSGD | 0.5000 | 0.0030 | - | - |
| | TA-MetaSGD* | 0.0349 | 0.0008 | 0.0001 | - |
| | MetaLSTM | - | 0.005 | - | - |
| | MetaLSTM++ | - | 0.0010 | - | - |
| | TA-MetaLSTM++* | - | 0.0002 | 0.0074 | - |
| | ANIL | 0.5000 | 0.0030 | - | - |
| | TA-ANIL* | 0.2826 | 0.0003 | 0.0024 | - |
| 5.5 | MAML | 0.5000 | 0.0030 | - | - |
| | TAML | 0.5000 | 0.0030 | - | 0.0153 |
| | TA-MAML* | 0.2826 | 0.0003 | 0.0024 | - |
| | MetaSGD | 0.5000 | 0.0030 | - | - |
| | TA-MetaSGD* | 0.0349 | 0.0008 | 0.0001 | - |
| | MetaLSTM | - | 0.005 | - | - |
| | MetaLSTM++ | - | 0.0002 | - | - |
| | TA-MetaLSTM++* | - | 0.0007 | 0.0003 | - |
| | ANIL | 0.5000 | 0.0030 | - | - |
| | TA-ANIL* | 0.2826 | 0.0003 | 0.0024 | - |
| 10.1 | MAML | 0.5000 | 0.0030 | - | - |
| | TAML | 0.5000 | 0.0030 | - | 0.0794 |
| | TA-MAML* | 0.2353 | 0.0002 | 0.0001 | - |
| | MetaSGD | 0.5000 | 0.0030 | - | - |
| | TA-MetaSGD* | 0.2583 | 0.0029 | 0.0007 | - |
| | MetaLSTM | - | 0.005 | - | - |
| | MetaLSTM++ | - | 0.0021 | - | - |
| | TA-MetaLSTM++* | - | 0.0005 | 0.0014 | - |
| | ANIL | 0.5000 | 0.0030 | - | - |
| | TA-ANIL* | 0.2826 | 0.0003 | 0.0024 | - |
| 10.5 | MAML | 0.5000 | 0.0030 | - | - |
| | TAML | 0.5000 | 0.0030 | - | 0.0193 |
| | TA-MAML* | 0.2353 | 0.0002 | 0.0001 | - |
| | MetaSGD | 0.5000 | 0.0030 | - | - |
| | TA-MetaSGD* | 0.2583 | 0.0029 | 0.0007 | - |
| | MetaLSTM | - | 0.005 | - | - |
| | MetaLSTM++ | - | 0.0004 | - | - |
| | TA-MetaLSTM++* | - | 0.0004 | 0.0090 | - |
| | ANIL | 0.5000 | 0.0030 | - | - |
| | TA-ANIL* | 0.2826 | 0.0003 | 0.0024 | - |

| Setting | Model | base lr | meta lr | attention lr | lambda |
|-----------------------|----------------|---------|---------|--------------|--------|
| tieredImageNet | | | | | |
| 5.1 | MAML | 0.5000 | 0.0030 | - | - |
| | TAML | 0.5000 | 0.0030 | - | 0.3978 |
| | TA-MAML* | 0.0261 | 0.0005 | 0.0015 | - |
| | MetaSGD | 0.5000 | 0.0030 | - | - |
| | TA-MetaSGD* | 0.0944 | 0.0003 | 0.0002 | - |
| | MetaLSTM | - | 0.005 | - | - |
| | MetaLSTM++ | - | 0.0002 | - | - |
| | TA-MetaLSTM++* | - | 0.0010 | 0.0006 | - |
| | ANIL | 0.5000 | 0.0030 | - | - |
| | TA-ANIL* | 0.0261 | 0.0005 | 0.0015 | - |
| 5.5 | MAML | 0.5000 | 0.0030 | - | - |
| | TAML | 0.5000 | 0.0030 | - | 0.7733 |
| | TA-MAML* | 0.0261 | 0.0005 | 0.0015 | - |
| | MetaSGD | 0.5000 | 0.0030 | - | - |
| | TA-MetaSGD* | 0.0944 | 0.0003 | 0.0002 | - |
| | MetaLSTM | - | 0.005 | - | - |
| | MetaLSTM++ | - | 0.0009 | - | - |
| | TA-MetaLSTM++* | - | 0.0012 | 0.0001 | - |
| | ANIL | 0.5000 | 0.0030 | - | - |
| | TA-ANIL* | 0.0261 | 0.0005 | 0.0015 | - |
| 10.1 | MAML | 0.5000 | 0.0030 | - | - |
| | TAML | 0.5000 | 0.0030 | - | 0.4752 |
| | TA-MAML* | 0.0821 | 0.0002 | 0.0006 | - |
| | MetaSGD | 0.5000 | 0.0030 | - | - |
| | TA-MetaSGD* | 0.0512 | 0.0007 | 0.0018 | - |
| | MetaLSTM | - | 0.005 | - | - |
| | MetaLSTM++ | - | 0.0011 | - | - |
| | TA-MetaLSTM++* | - | 0.0018 | 0.0002 | - |
| | ANIL | 0.5000 | 0.0030 | - | - |
| | TA-ANIL* | 0.0821 | 0.0002 | 0.0006 | - |
| 10.5 | MAML | 0.5000 | 0.0030 | - | - |
| | TAML | 0.5000 | 0.0030 | - | 0.2501 |
| | TA-MAML* | 0.0821 | 0.0002 | 0.0006 | - |
| | MetaSGD | 0.5000 | 0.0030 | - | - |
| | TA-MetaSGD* | 0.0512 | 0.0007 | 0.0018 | - |
| | MetaLSTM | - | 0.0050 | - | - |
| | MetaLSTM++ | - | 0.0024 | - | - |
| | TA-MetaLSTM++* | - | 0.0015 | 0.0019 | - |
| | ANIL | 0.5000 | 0.0030 | - | - |
| | TA-ANIL* | 0.0821 | 0.0002 | 0.0006 | - |